GCB Bioenergy

WILEY

Global Change Biology Bioenergy
BIOPRODUCTS FOR A SUSTAINABLE BIOECONOMY

RESEARCH ARTICLE OPEN ACCESS

Drought Response in *Miscanthus*: Breeding Increases Radiation and Water Use Efficiency Over Three Contrasting Years in Central Germany

Danny Awty-Carroll[1,2] | Paul R. H. Robson[1] | Kai-Uwe Schwarz[3] | Heike Meyer[3] | Jörg Michael Greef[3] | Astley Hastings[4] | John Clifton-Brown[1,5]

[1]Institute of Biological, Environmental and Rural Sciences (IBERS), Aberystwyth University, Aberystwyth, Wales, UK | [2]School of Biological and Environmental Sciences, Faculty of Science, Liverpool John Moores University, Liverpool, UK | [3]Julius Kühn-Institut (JKI), Federal Research Centre for Cultivated Plants, Braunschweig, Germany | [4]Institute of Biological and Environmental Science, University of Aberdeen, Aberdeen, UK | [5]Department of Agronomy and Plant Breeding I, Research Centre for Biosystems, Land Use and Nutrition (iFZ), Justus Liebig University Giessen, Giessen, Germany

Correspondence: John Clifton-Brown (john.clifton-brown@agrar.uni-giessen.de)

Received: 31 May 2025 | **Revised:** 23 September 2025 | **Accepted:** 24 September 2025

Funding: Danny Awty-Carrol was supported by the UK Biotechnology and Biological Sciences Research Council (BBSRC) through the GIANT-LINK (LK0863 with DEFRA), MUST (BB/N016149/1, also with DEFRA) and OMENZ (TER-303-1-M with BEIS) projects. Paul Robson was supported by the EU projects Development of improved perennial non-food biomass and bioproduct crops for water-stressed environments (WATBIO, 311922) and Optimizing Miscanthus Biomass Production, OPTIMISC, 289159) and the BBSRC Strategic Programme for Resilient Crops (grants BB/K01711X/1 BBS/E/IB/230001C BB/CSP1730/1). Kai Schwarz, Heike Meyer and Jörg Greef were supported by WATBIO, Fachagentur Nachwachsende Rohstoffe (FNR), Bundesministerium für Ernährung und Landwirtschaft (Züchtung neuer samenvermehrter Miscanthus-Hybriden, 22016016) and the Julius Kühn-Institute. Astley Hastings was funded by the UKRI PCB4GGR (BB/V011553/1) and UKERC-4 projects. John Clifton-Brown was supported by OPTIMISC, WATBIO, GIANT, MUST and FNR projects and during the write up phase in 2025 by the European Innovation Partnership for Productivity and Sustainability in Agriculture (EIP-Agri) project: Integration of perennial Miscanthus strips on arable land, Regierungspräsidium Gießen, Project number 9100447-Invest-1.

Keywords: bioenergy | breeding | drought | energy crops | *Miscanthus* | process modelling | radiation use efficiency | water use efficiency

ABSTRACT

More and new sources of biomass are needed for renewable energy and renewable products for the bioeconomy. A leading new source of biomass is the highly sustainable perennial grass crop Miscanthus. The majority of the Miscanthus crop comprises a clone of *Miscanthus* × *giganteus* (*M*×*g*) of limited genetic variation and poor yield under dry growth conditions. The parental species of *M*×*g*, *M. sacchariflorus* and *M. sinensis*, are distributed over a large geographical range in Eastern Asia and may be used to improve on *M*×*g*. From breeding trials, we selected seven novel hybrids and two control genotypes including *M*×*g*. We grew these in a field experiment on drought-prone soil in Germany with and without irrigation. To identify superior Miscanthus types, we estimated radiation use efficiency (RUE), yield and water use efficiency (WUE) from within-season measurements made over three contrasting growing seasons. Temporal variations in RUE and WUE for different genotypes varied significantly and two novel hybrids, WAT6 and WAT8, achieved the highest yields. To achieve goodness of fit to yield measurements, genotype-specific parameters for process descriptions in the model MiscanFor were adjusted for the two superior genotypes. These parameters included earlier shooting and an increased threshold of overheating. When the model was run over ten years, despite generating the highest yield values, WAT8 accumulated less biomass than WAT6 over the longer term. The response of WUE to variation in soil capillary pressure and vapour pressure deficit was examined. WUE of *M*×*g* increased with the severity of water stress then

Danny Awty-Carroll and Paul R.H. Robson contributed equally to the manuscript.

declined again. The superior yielding genotypes were more able to sustain biomass accumulation and/or water use under the highest stress. We believe that combining physiology with crop modelling is a powerful way to inform genetic and agronomic improvements needed to secure the future supply of biomass for the bioeconomy.

1 | Introduction

Weather extremes resulting from global warming are changing the temporal and spatial availability of water resources for crop growth (Dietz et al. 2021). Under drought conditions, crops with C_4 photosynthesis have the potential to achieve higher yields than the more common C_3 plants (Taylor et al. 2014). The 'Saccharum complex' of C_4 grasses, which includes sugarcane, maize, sorghum and several other perennial grass species that can interhybridise (Shanmuganathan and Sudhagar 2021), is of increasing importance for food and non-food biomass (Al-Salman et al. 2024; FAO 2024; Smith and Boardman 2025). *Miscanthus* is genetically a 'doubled sorghum' (Ma et al. 2012). However, *Miscanthus* has two unique features: perennialism and an especially low temperature-adapted C_4 photosynthesis (Naidu et al. 2003). *Miscanthus* regrows annually from its rhizome, which provides efficient nutrient recycling and due to a lack of regular soil tillage, soil organic carbon accumulates and soil erosion is lessened (Cosentino et al. 2015). In side-by-side field trials with maize, *Miscanthus* achieved higher dry matter biomass yields than maize (Dohleman and Long 2009), and when the energy input (in fertiliser, pest control, etc.) and outputs (biomass) are compared, then *Miscanthus* has a far superior (lower) input: output ratio (Kiesel et al. 2016). The high yields and efficiencies have resulted in sustained research and commercial interest in *Miscanthus* as a source of biomass over many decades.

To explore the potential for genetic improvement of *Miscanthus* to increase yield, quality and adaptive range, breeding endeavours were set up independently and in collaboration in Europe, Asia and the US (Clifton-Brown et al. 2017). Most of these breeding endeavours involve the collection and characterisation of wild *Miscanthus* germplasm from its origins in Eastern Asia (Hodkinson et al. 2016). Several species that can hybridise are found over a very wide range of climates, latitudes and altitudes (Huang et al. 2019). The most famous *Miscanthus* is an interspecies hybridisation from Japan (Nishiwaki et al. 2011) of *M. sacchariflorus* and *M. sinensis* known as *Miscanthus* × *giganteus* (*M*×*g*) (Greef and Deuter 1993). Field trials in central Europe (Kalinina et al. 2017), in the Midwest of the USA (Heaton et al. 2009) and Northern Japan (Nakajima et al. 2018) have shown that *M*×*g* is remarkably widely adapted and can achieve high yields where there is sufficient soil moisture during the growing season. However, in summers with prolonged droughts on soils with a low water holding capacity, mature spring harvestable yields can fall from >12 to <3 t DM ha^{-1} (Clifton-Brown et al. 2019). High yield and yield stability in locations and years with water deficits is an important breeding objective. Performance improvement under water deficits is controlled by a combination of physiological processes; therefore, breeding for single traits is unlikely to achieve significant improvements. So, we took a hybrid breeding approach, crossing diverse accessions of *M. sacchariflorus* and *M. sinensis* parents from different origins in Asia (Huang et al. 2019) using geographic diversity as a proxy for the essential genetic diversity needed in breeding programmes (Swarup et al. 2021). We hypothesised that by either intra and interspecies crossing, novel *Miscanthus* hybrids could be bred with higher yield potentials and higher yield stability in both dry and wet years. To this end, nine promising genotypes were selected in 2014 to be grown in a field trial with rainfed and irrigated treatments in JKI Braunschweig. The aims of the trial were to compare the growth performances in terms of canopy light interception, radiation use efficiency and water use efficiency. These are the key parameters in crop models used to predict yield performance.

Crop models play a crucial role in understanding plant responses to various environmental variables. MiscanFor is a dynamic, process-based model specifically designed to simulate the growth, development and yield of *Miscanthus* crops coded in FORTRAN (Hastings et al. 2009b). This model evolved from the MISCANMOD framework (Clifton-Brown et al. 2000) and was parameterized and validated using field trials conducted across Europe (Clifton-Brown et al. 2004). MiscanFor integrates multiple environmental and management factors, including soil properties, weather conditions and agricultural practices, to provide accurate predictions of biomass production by incorporating detailed physiological processes such as photosynthesis, respiration and water-use efficiency. MiscanFor has been instrumental in predicting how *Miscanthus* responds to various environmental scenarios (Hastings et al. 2009a; Hastings et al. 2014). The ability to simulate long-term crop performance under changing climatic conditions is particularly valuable (Hastings et al. 2009a; Pogson et al. 2013; Littleton et al. 2020; Shepherd et al. 2020; Zhang et al. 2020a, 2020b). The model has been parameterized for several different *Miscanthus* genotypes (Shepherd et al. 2023). Key processes modelled within MiscanFor include germination, shoot emergence, flowering and senescence. Additionally, it incorporates a soil–plant water model that utilizes soil physics to calculate soil capillary pressure (Campbell 1985). The model also employs the Penman-Monteith equation for calculating potential evapotranspiration (Monteith 1965), alongside a water-use model that accounts for plant interception, soil evaporation, plant transpiration and runoff/leaching. This comprehensive approach makes MiscanFor particularly well-suited for modelling the responses of *Miscanthus* to drought conditions and for assessing yield profiles. Moreover, trial results can be compared with predicted yield values derived from MiscanFor's simulations, providing valuable parameterization applicable to a broader range of genotypes.

The specific objectives of this study were to compare in nine different *Miscanthus* genotypes, selected from breeders' plots, grown over three years with and without irrigation on a drought-prone sandy soil in Central Germany: (1) the dynamics of canopy light interception and conversion (LI, RUE, respectively) with and without water deficits, (2) the WUE in terms of biomass per unit of evapotranspired water of different treatments and (3) the yield and yield stability. The expected impacts of this study include (a) the identification of higher-performing genotypes resulting from breeding to date,

TABLE 1 | Details of the *Miscanthus* genotypes used in the trial. *M. sinensis* (*M. sin*), *M. sacchariflorus* (*M. sac*).

Name	Species	Origin	Ploidy
WAT3	*M. sac*	Japan	Tetraploid
WAT4	*M. sac* (Robustus)	China	Diploid
Goliath	*~M. sin* × *~M. sin*	Unknown	Triploid
WAT5	*M. sin* [×2] × *M. sac* [×4]	Taiwan × Japan	Diploid
WAT6	*M. sac* (Robustus) [×2] × *M. sin* [×2]	China × Japan	Diploid
WAT7	*M. sac* (Robustus) [×2] × *M. sin* [×2]	China × Japan	Diploid
WAT8	*M. sac* (~Robustus) [×2] × *M. sin* [×2]	China × ~Japan	Diploid
WAT10	*M. sac* (Robustus) [×2] × unknown	China × unknown	Diploid
WAT9 (*M*×*g*)	*M. sac* × *M. sin*	Japan × Japan	Triploid

Note: Ploidy is shown in square brackets for the maternal and paternal parents. The control genotype '*M*×*g*' is the clone of *M.* × *giganteus*. ~ indicates inference rather than from direct records.

(b) using the dynamic responses measured to improve modelled yield potentials grown under different environments and (c) informing further breeding of high-yielding and resilient *Miscanthus* varieties.

2 | Materials and Methods

2.1 | Study Site

The location of the experiment was Julius Kuhn Institute, Braunschweig (52°17′59″ N—10°26′16″ E, altitude 76 m) in Northern Germany. The soil type is a Haplic Luvisol (FAO 1994). Over a soil depth of 150 cm, the soil texture comprises 79% sand, 16% silt and 6% clay. It has a bulk density of 1.59 g cm^{-3} and large pore volume of 24%. The topsoil to 60 cm is silty to loamy sand, below which is pure sand. The plant available water holding capacity (0–1.5 MPa) of the top 100 cm was estimated at 150 mm (Frank Höppner, pers. comm). Daily weather data for maximum and minimum temperature, relative humidity (at 9 am), global radiation, precipitation and wind run were provided for the Braunschweig site by the German Weather Service (Deutsche Wetter Dienst, DWD). Daily atmospheric Vapour Pressure Deficit (VPD) was calculated using the 9 am temperature and relative humidities.

2.2 | Genotype Origins, Selection and Breeding

Wild Asian Miscanthus collections were phenotypically selected in field trials in Europe for use in breeding (Clifton-Brown et al. 2019). We hypothesised that interspecific crossing with diverse selections and complementary traits could produce higher yielding and more resilient hybrids. From our breeding nurseries, two wild and five hybrid genotypes covering different origins, species and ploidy (Table 1) were carefully selected for this study. These were compared to two triploid commercial clones, the intraspecific hybrid 'Goliath' and the standard interspecific hybrid *Miscanthus*×*giganteus* (*M*×*g*) (Greef and Deuter 1993). The study was part of the EU project WATBIO (2013–2017), and therefore all genotypes have the prefix 'WAT'.

WAT3 is a selection from wild sourced Japanese *M. sacchariflorus* from Shikoku Island and is a similar type to the *M. sacchariflorus* parent that created standard *M*×*g*. WAT4 is a halophyte selection of *M. sacchariflorus* type known as 'Robustus'. It was collected in China near Dongying city, which is in the Yellow River Delta. It is an area of such high salinity that there is salt deposition on the soil surface. Goliath (*M. sinensis*, cv. Goliath) is officially origin unknown. It is likely to have been selected from an open pollination from a maternal tetraploid and a paternal diploid, both *M. sinensis*. It may have been selected by the horticultural breeder Ernst Pagels (Oldenburg, Germany), who was active in the 1960s and who produced many of the ornamental *Miscanthus* genotypes that are widely traded in garden centres throughout Europe. WAT5's maternal parent is a diploid *M. sinensis* from the upland 'Alishan' mountain region in Taiwan. Its paternal parent is a tetraploid from Kumamoto in Japan and is of a similar type to WAT3. WAT6's maternal line is a diploid Chinese *M. sacchariflorus* genotype of the type 'Robustus', similar to WAT4. WAT6's paternal line is a diploid *M. sinensis* from the Nagano region in Japan. WAT7's maternal line is a diploid *M. sacchariflorus* (similar to WAT4) from Lake Khanka in China, and its paternal line is a diploid *M. sinensis* from central Japan (MS88-110 also known as EMI-11 (Clifton-Brown et al. 2001)). WAT10 (also known as 'BS75') arose from open pollination of a Chinese Robustus genotype similar to WAT4 in Braunschweig, Germany. *M*×g, which is the standard commercial *Miscanthus*, is a naturally occurring open-pollinated hybrid of tetraploid *M. sacchariflorus* and *M. sinensis* collected from Japan (Linde-Laursen 1993; Stewart et al. 2009). Previous field trials in Braunschweig had shown that *M*×*g* was high yielding in wet years but produced much less in dry years (e.g., 2003), when yields from Goliath exceeded those of *M*×*g* (Kai Uwe-Schwarz, pers. comm.).

To produce sufficient stocks for replicated plot trials all nine clonal genotypes were initially propagated by in vitro tillering and planted in the field in 2012. In 2014, all nine selected genotypes were rhizome propagated by splitting the well-developed plants into equal portions to produce 128 plants (16×8) per genotype. These were grown under rainfed conditions for a further two years, before bi-monthly phenotyping began in 2016.

2.3 | Experimental Design

The experimental site was established in 2014 with eight blocks: four blocks were alternately assigned to rainfed and irrigated treatments. Within each block, nine 8 m^2 plots were planted, each containing a randomly assigned genotype. Within each plot, 16 plants were planted at a density of 2 plants m^2, matching earlier EU projects (Clifton-Brown et al. 2001; Kalinina et al. 2017). To ensure uniform establishment, all plants were propagated from equally sized propagules. To minimise edge effects and reduce the risk of soil variations between genotypes and the irrigation treatments, plots were planted adjacent to each other, omitting only one row between the plots. Following planting, all plants were watered to ensure hydraulic contact with the soil. Thereafter, all eight blocks were rainfed for two growing seasons to allow the *Miscanthus* plants to fully establish, achieving gap-free homogeneous plots. From 2016, irrigation was applied to four of the blocks using drip lines (Netafim Ltd., Tel Aviv, Israel) laid between each row of plants.

Weather data published by the German Weather Service (DWD, Braunschweig) was used to calculate a water balance between the incoming rainfall and the outgoing evaporation estimated by the Penman-Monteith equation (Allen et al. 1998). The target irrigation level was between 80% and 100% of modelled evaporation. In addition to the modelling of soil moisture deficits, twelve reflectometers (CS615, Campbell Scientific Ltd., Leicestershire, UK) were also installed under six plots at 25 and 75 cm to monitor directly the changes in soil moisture content under irrigated and rainfed plots of three different genotypes.

2.4 | Phenotyping

Measurements of plant height, canopy light interception, flowering time and standing biomass were made in three consecutive growing seasons, 2016–2018. These were used to identify key phenophases (Dietz et al. 2021) such as emergence and flowering time, and to quantify the impacts of water deficits on growth using the differences between irrigated and rainfed treatments. A brief description of the phenotyping protocol for each measurement parameter follows:

Plant height was measured approximately weekly during the growing season on a marked shoot from the ground up to the youngest leaf ligule in a centrally positioned plant to the nearest centimetre. In spring and autumn, measurement intervals ranged between 2 and 4 weeks. Shoot counts per plant were made on the same plant as the height measurements. To avoid including shoots that are not contributing appreciably to the standing biomass, shoots were only counted that were within 60% of the plant height (also known as 'canopy contributing shoots') (Magenau et al. 2022).

Canopy light interception was measured using a 1 m long 'ceptometre' array of photodiodes (10) connected to an amplifier to give a linear response to Photosynthetically Active Radiation, as described in Nunn (2017) and further described in the 'Modelling' section. Incident radiation was measured outside the plots immediately before and after measurement of the transmitted radiation under the crop canopy. Measurements were made between 10 and 14 h under both clear and overcast skies as they occurred on the scheduled measurement date.

Green leaf area on one marked shoot per plot was determined by measuring the length and the width of every green leaf on the shoot. As the older leaves senesced, their contribution to the green leaf area was removed. The green leaf lengths and widths were multiplied by a previously derived coefficient of 0.7 (Clifton-Brown 1997) to calculate the green leaf area in cm^3. A green leaf area index (LAI) was calculated from the product of the shoot counts (m^{-2}) and the green leaf area of the shoot.

Visual flowering scores used a 0–5 scale with a score of 1 indicating the beginning of anthesis through the appearance of a flag leaf, 2 indicating the emergence of the panicle from the leaf sheath, 3 indicating anthesis has started, 4 indicating the flower has fully emerged with mature stigmas and anthers visible and 5 indicating the end of flowering (Awty-Carroll et al. 2024).

As *Miscanthus* is perennial, it is not possible in small (8 m^2) plots to cut quadrats throughout the growing season to determine the dynamics of yield without impacting growth and yield in the same and subsequent years. Therefore, we used a less damaging method based on serial cuts of a small number of shoots which were related by ratio to the final harvest yield determined by harvesting biomass within quadrats. We have used this approach successfully several times though the size of the samples varied slightly depending on the research questions (Nunn et al. 2017; Magenau et al. 2022; Shepherd et al. 2023). In this study, at every date in the growing season when the standing crop biomass was to be determined, one randomly selected shoot per plant on a pre-determined plant was removed for mass determination. The random shoot selection was performed using a line transect approach by inserting a stick with two marks on it, one to align with the planting grid and a second used to identify the shoot that fulfilled the criteria of 60% of the plant (canopy) height (as for the shoot counts above) nearest to the mark. At each serial cut the sampled shoot was cut from a different plant to minimise the damage to any particular plant. The cut shoot dry weight was determined by oven drying to constant weight at 80°C. To estimate the standing yield, shoot dry weights were multiplied by the final count of shoots contributing to the canopy. At the final harvest in spring, following winter ripening (as is normal for *Miscanthus* (Lewandowski and Heinz 2003)), a quadrat harvest was performed on the central 4 plants (2 m^2) in each plot in February–March 2017, 2018 and 2019.

2.5 | Modelling

Raw phenotypic data collected with the protocols as described in the previous section were combined with the meteorological data to derive the dynamics of intercepted radiation (Light interception by the canopy), radiation use efficiency (RUE) and water use efficiency (WUE), key parameters for crop modelling.

A reading of the incident radiation was made using the ceptometer above the canopy (A_0) before readings of the transmitted radiation were made below the canopy in four positions each 90°

from each other (B_N, B_E, B_S and B_W), followed by another measurement of the incident radiation above the crop (A_1). Light interception (I) was calculated as the fraction of light intercepted by the leaf canopy using Equation (1).

$$I = 1 - \frac{\left(\frac{B_N + B_E + B_S + B_w}{4}\right)}{\left(\frac{A_0 + A_1}{2}\right)} \quad (1)$$

The accumulated energy (E) intercepted by the plant at time t is the proportion of intercepted (I) multiplied by the global radiation (G) from the weather station until that point. A simple binomial line was fitted to give the energy intercepted at every day of the year.

$$\mathrm{RUE}_t = \frac{M_t}{E_t} = \frac{M_t}{\sum_{i=1}^{t} [I_i \cdot G_i]} \quad (2)$$

Radiation-use efficiency was calculated by dividing aboveground biomass (M) of each plot calculated from the standing crop yields at each time point (t) by the accumulated energy intercepted by the plant (E) at time t (Equation 2).

$$WUE_t = \frac{M_t}{\sum_{i=1}^{t} R_i + W_i} \quad (3)$$

Water-use efficiency was calculated from the standing crop yields (M) divided by the accumulated rainfall (R) plus, in the irrigated plots, accumulated irrigation (W) at each time t (Equation 3). This basic water-use efficiency was compared with the water-use efficiency calculated in MiscanFor (Hastings et al. 2009b), which estimates daily evaporation, runoff and transpiration using methods described in Allen et al. (1998) and Holder et al. (2018) and is presented in Figure 1.

The MiscanFor model (Hastings et al. 2009b) initially was parameterised with $M \times g$, principally with data collected in 1994 and 1995 in Ireland (Clifton-Brown et al. 2000). Over the years, additional parameters were added to better account for the impacts of water deficit, the temperature of leaf formation and photosynthesis, switches for shooting, leaf formation, flowering and senescence, overheating and overwinter frost tolerance using data from controlled environment experiments and multi-location trials (Nunn et al. 2017; Shepherd et al. 2023). Additionally, the site-specific derived soil characteristic Plant Available Water (PAW) was included. When

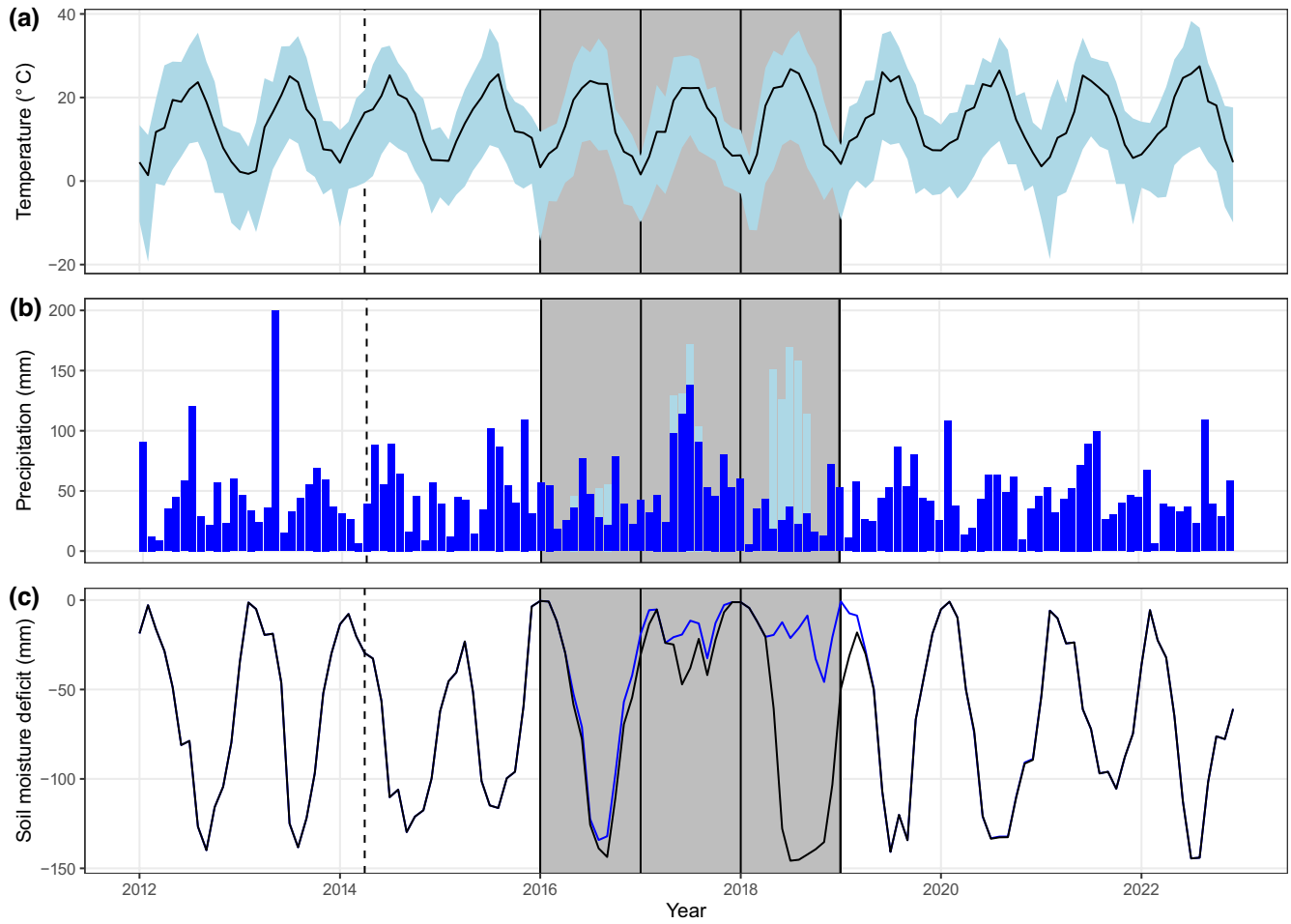

FIGURE 1 | Daily weather recorded at the DWD Braunschweig station from 2012 to 2022. (a) Average, minimum and maximum monthly temperatures. (b) precipitation with light blue bars showing supplemental irrigation added to the irrigated plots. (c) Calculated values for soil moisture deficit with the black and blue lines for the rainfed and irrigated treatments respectively. A dotted line represents the date of planting and the shaded area the years of intensive measurements.

soil moisture deficits fell below field capacity of the soil water, a curve based on the soil water release curve (capillary pressure) for the sandy soil and the leaf area index was used to estimate the actual evaporation from the potential evaporation (Campbell 1985).

The existing model parameters for $M\times g$ were used to model the $M\times g$ trials from 2016 to 2018 for both the irrigated and the rain-fed plot trials and validated using the actual yield and phenotype data gathered in this project. New parameters for two of the leading genotypes (WAT6 and WAT8) were required because of their higher yield than $M\times g$ in this trial and were developed from the phenotype data and incorporated into the model. This was achieved by comparing the phenological measurements described in this paper of the new genotypes to those of $M\times g$ and using these differences to modify the triggers, rates and brakes in the model. Triggers and brakes are degree-day, temperature and soil water parameters that specify the start and stop of each phase of plant growth such as shoot emergence, leaf expansion, flowering, senescence and ripening. These are represented in the model by the phenotypical parameter called 'physiostat' and this was adjusted to match the observed degree days above optimised base temperatures at each stage for each genotype. Rates relate to leaf expansion and photosynthesis rates, which are modified by temperature and available water. Temperature sensitivity relates to the actual temperature of the start of growth and the change in RUE with increasing temperature and an 'overheat' temperature threshold at which RUE declines. This was facilitated by the contrasting climatic conditions of the three years for both the rainfed and irrigated experiments. The model uses the capillary pressure of the remaining soil water to modify and reduce the RUE as the soil dries. Using the irrigated and rainfed experimental observations, the different response of the WAT6 & 8 to $M\times g$ genotypes allowed the threshold of RUE reduction to be determined for each.

The updated model with the Braunschweig site specific soil parameters (Field Capacity and Wilt Point) was run for three genotypes $M\times g$, WAT6 and WAT8 using ten years of meteorological data from 2012 to 2022, providing modelled data from four years before and three years after the measurement years (2016–2018). Where the observed data overlaps with the modelled data, these were plotted together to evaluate the model performance in predicting soil moisture content, growth and transpiration/water use (though not in an independent way). The performance of the three genotypes was compared over the period 2012–2022 to evaluate the total biomass potential of each at the Braunschweig site using the meteorological data recorded by the German Weather Service.

2.6 | Data Analysis

Microsoft Excel was used for the phenotyping data capture and for the Penman-Monteith evapotranspiration (ET) in a spreadsheet developed by the Cranfield University hydrologists Tim Hess and William Stephens for the assessment of hydrological impacts of bioenergy crops (Stephens et al. 2001). All statistical analyses and data manipulation, including the calculation of stress indices, were conducted using R (R Core Team 2024). Graphical representations of data dynamics were generated using the ggplot2 package in R (Wickham and Sievert 2009).

To assess the effects of genotype, year and watering treatment, a three-way analysis of variance (ANOVA) was performed on final harvest dry weight yield and yearly water use efficiency, as well as maximum light interception and shoot heights just on or before the 1st of July. Prior to analysis, the assumptions of the ANOVA were verified. Homogeneity of variance was confirmed using Levene's test in the CAR package in R (Fox and Weisberg 2018) and normality of the residuals was assessed via the Kolmogorov–Smirnov test, as well as visual inspection with a Quantile–Quantile plot, histogram and boxplot. The light interception data was arcsine square root transformed as it is a percentage. Post hoc comparisons among genotypes were conducted using Tukey's Honest Significant Difference (HSD) test, utilizing the Agricolae package in R (Mendiburu 2019). Where a more detailed breakdown by year or genotype was required, estimated marginal means from the Emmeans package (Russell et al. 2018) were used with a Holm–Bonferroni applied.

Rankings and yield stress models were used to differentiate genotype yield stability under the drought conditions.

Table 2 shows the stress statistics calculated where Y is the yield in question under either control Y_c or drought Y_d and the $\overline{Y}$ is the mean of all yields under that condition.

3 | Results

3.1 | Weather Conditions

The three measurement years were subject to quite different climatic conditions. Broadly, there was a late season drought in 2016, very little detectable water stress in 2017, and a severe and protracted drought in 2018. Figure 1 shows the three measurement years in the context of interannual climatic variations over the period 2012–2022. The average annual

TABLE 2 | Three stress stability indices used to assess the yield stability of different genotypes grown with and without irrigation in three consecutive years.

Stress susceptibility index	$\mathrm{SSI} = \frac{1-\frac{Y_d}{Y_c}}{\left[1-\frac{\overline{Y_d}}{\overline{Y_c}}\right]}$	Fischer and Maurer (1978)
Stress tolerance index	$\mathrm{STI} = \frac{Y_c}{\overline{Y_c}}\frac{Y_d}{\overline{Y_d}}\frac{\overline{Y_d}}{\overline{Y_c}} = \frac{Y_c \cdot Y_d}{\overline{Y_c}^2}$	Fernandez (1992)
Yield stress score index	$\mathrm{YSSI} = \frac{(\mathrm{STI}+\mathrm{SSI})}{2}$	Thiry et al. (2016)

temperature in JKI over the 10 years was 10.5°C and ranged from a minimum of −19°C in winter to +38°C in summer (Figure 1). The measurement years for this trial, from 2016 to 2018, are indicated in grey. The average temperature for the measurement period was 10.6°C, which was like the 10-year mean.

The average annual rainfall over the 10-year period was 574 mm, and over the three measurement years was 567 mm (Figure 1). There was a large (2.5×) difference between the 818 mm in 2017 and the 318 mm in 2018. Figure 1 also shows the additional water applied to the irrigated treatment. Modelling the water balance daily with MiscanFor showed that the irrigation rates applied in 2016 were lower than the calculated evaporative demand Figure 1, but in 2017 and 2018, irrigation amounts were sufficient to meet the evapotranspiration demands of the crop.

Figure 2 shows in more detail the dynamics of the water deficits in the soil (modelled soil capillary pressure (CAP) (kPa)) and in the atmospheric demand (in terms of Vapour Pressure Deficit, VPD, in kPa). Figure 2 shows that at the end of July 2016, capillary pressures remained high until the end of the growing season in September. With a nearly optimal rainfall distribution throughout the growing season, 2017 was an unusually wet year. But 2018, which started with an early season water deficit, later developed into an unusually prolonged and severe whole season drought with higher VPDs than those recorded in the previous two years. The modelling of capillary pressure shows how effective the irrigation treatments were in ameliorating the potential for drought in 2018.

Direct measurements of the volumetric soil moisture contents made at two depths (25 and 75 cm) with soil water reflectometers under plots of three genotypes ($M\times g$, WAT3 and WAT10) (Figure S1) corroborated well with the modelled water balances for the rainfed and irrigated treatment over the three years (Figure 2). The soil moisture probes under the $M\times g$ and WAT10 plots detected no notable differences in the soil moisture content dynamics, but it was interesting to observe that in the irrigated treatment, WAT3 had consistently higher volumetric soil water contents (individual genotype data not shown).

3.2 | Growth Dynamics

Figure 3 shows the fortnightly progression of shoot height in 2016, 2017 and 2018, and an additional horizontal line shows when flowering occurs. In 2016, growth in the rainfed $M\times g$ plots stopped in early August, but irrigation helped to maintain growth rates, though there was a significant dip in growth rates in late August indicating the water supplied by the irrigation was insufficient to keep up with this genotype's demand for water. The newer genotypes also showed significant differences in the dynamics of height between the irrigated and rainfed treatments, but the differences were less than with $M\times g$. In the wet year of 2017, shoot height ranged from 1.8 to 2.8 m, with

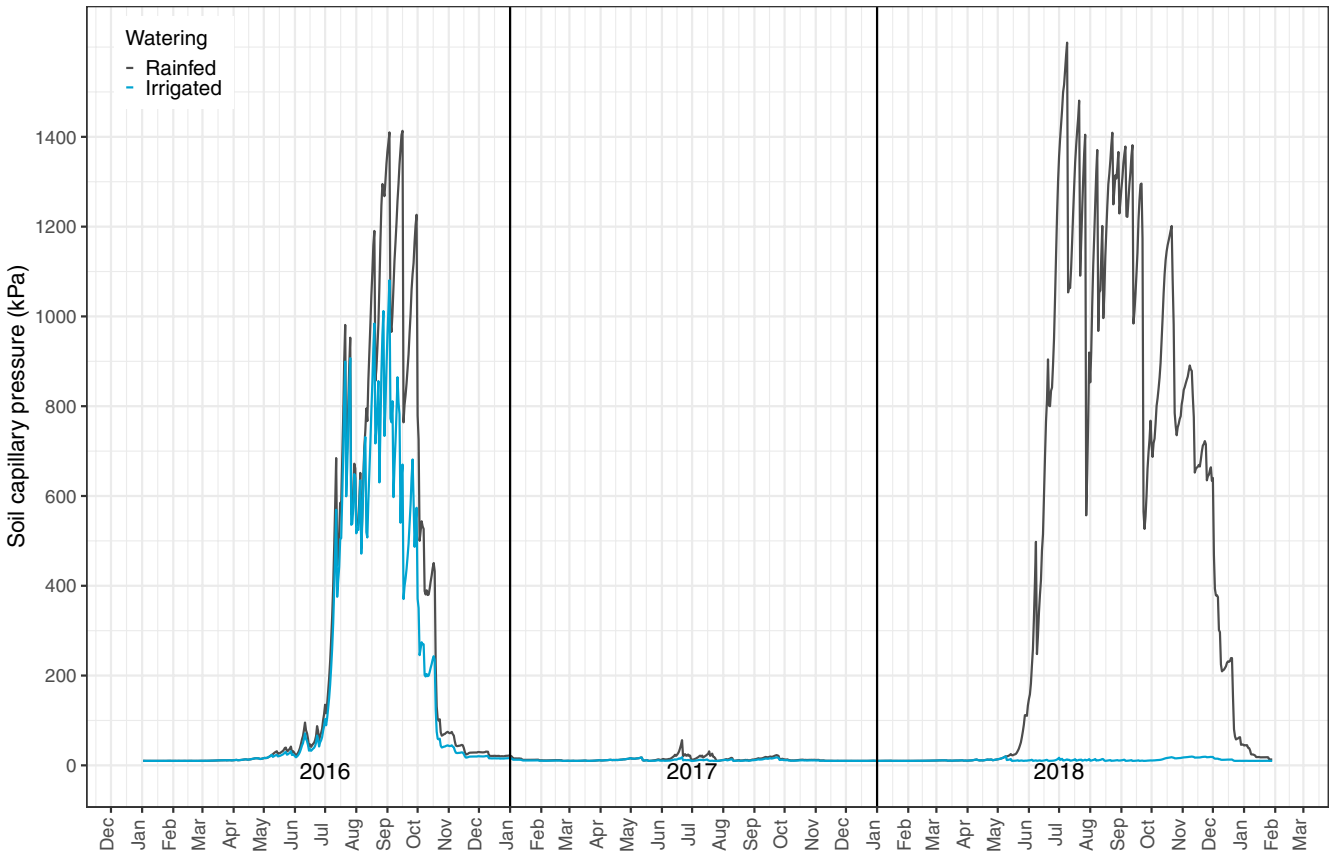

FIGURE 2 | Weekly mean values of vapour pressure deficit (dotted line) and soil capillary pressure (solid lines). Both as calculated from daily meteorological data from the JKI Braunschweig site with soil capillary pressure modelled with the assumption that 150 mm of water was available to the plant in the top 1 m (Blue line is irrigated and black line is rainfed).

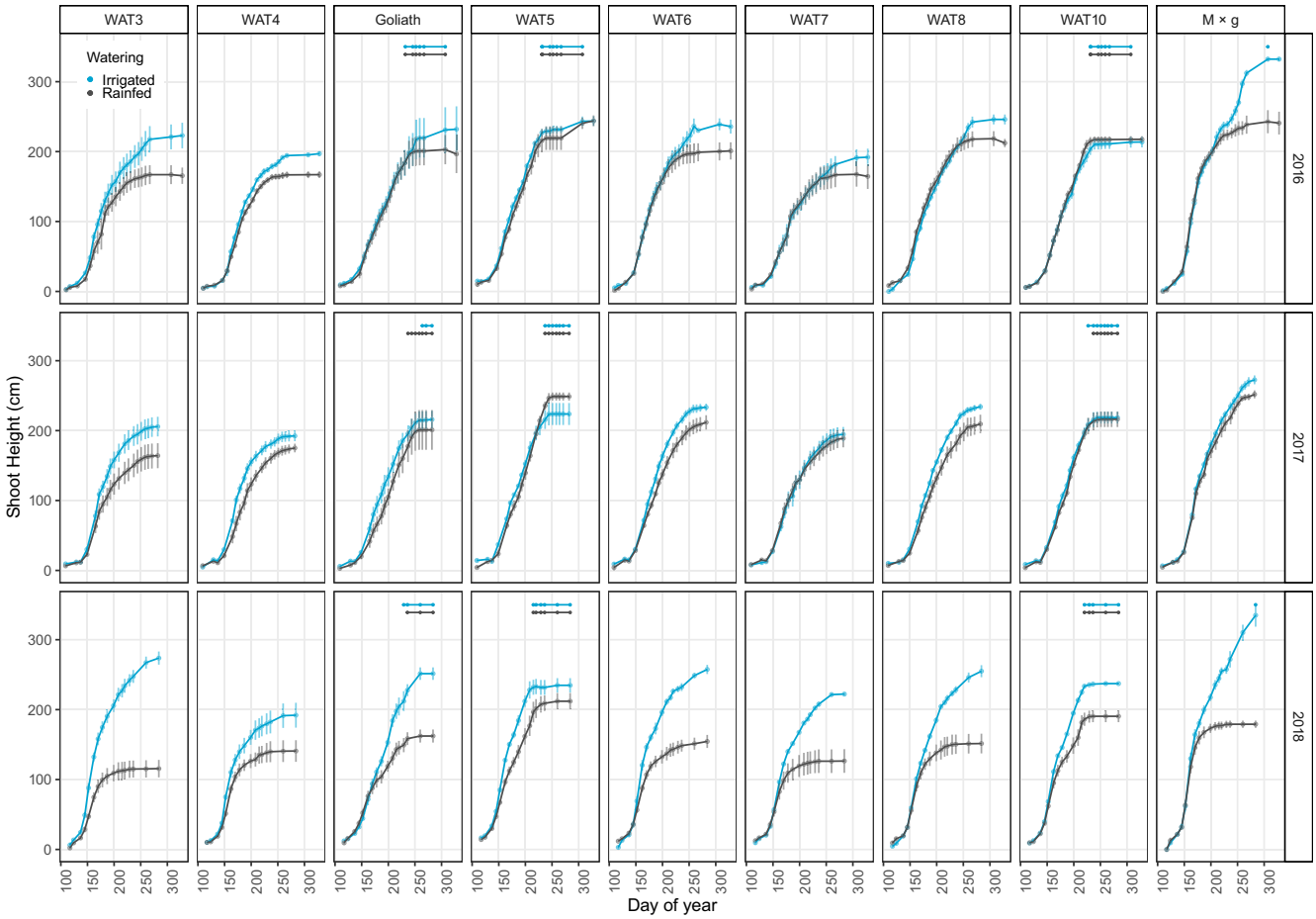

FIGURE 3 | Progressions of shoot height in 2016, 2017 and 2018 for 7 novel Miscanthus genotypes and the controls $M \times g$ and Goliath in the WATBIO trial at JKI Braunschweig. Dates for the duration of plant flowering are marked with a horizontal line at the top. Error bars ±1 SE, $n = 4$.

additional irrigation making a small but significant impact on height for 7 out of 9 genotypes. In 2018, the early and then prolonged drought resulted in large height differences in all genotypes except WAT5. From the shape of the curves in Figure 3 the irrigation amounts in 2018 kept up with the demands of $M \times g$, which is also supported by the soil moisture levels measured at 25 cm (Figure S1).

$M \times g$ only flowered at the end of the growing season in hotter years, so flowering did not affect growth. However, in WAT10, WAT5 and Goliath, the effect of flowering can be seen clearly in the height data (Figure 3). $M \times g$ showed the most significant effect of irrigation on height in the two years with water limitation, though all genotypes apart from WAT5 had a clear reduction in height from the 2018 drought.

The genotypes with the lowest number of leaves per shoot were WAT5 and WAT10 (~15 leaves), and the genotypes with the highest (> 20) were WAT3, WAT8 and $M \times g$ (Figure 4A). During the late-season drought in 2016, irrigation increased the number of leaves in WAT7, but there was very little response in terms of leaf numbers from the other genotypes. In contrast, green leaf duration (leaf lifespan) in 2016 was highest in WAT8 in the irrigated treatment, and there appeared to be a slight delay in the timing of successive leaves associated with the higher water availability. In 2017, with only mild water stress, there were more leaves per shoot and the green leaf durations were longer than in 2016. Exceptionally, the genotype Goliath produced an extra 5 leaves with irrigation in 2017. A similar response was not seen in 2016, which is probably due to differences in the water supply at different phenostages.

The green leaf area index (GLAI) (Figure 4B), estimated from the sum of all the areas of the green leaves (Figure 4A) multiplied by the count of the shoots per m^2 that were contributing to the canopy (Figure S2), ranged from 0 at the beginning of the growing season to > 16 at peak in early August.

Although WAT4 has shorter shoots and lower leaf areas per shoot, this genotype had consistently the highest GLAI in both years with and without irrigation on account of its high shoot counts (Figure S2). WAT8 reached high GLAIs, particularly in the irrigated treatments in both years and also in the rainfed treatment. Although these detailed measurements were not continued in 2018, the GLAIs recorded in 2016 and 2017 for all these *Miscanthus* genotypes were well above the canopy closure GLAI of 4, which is needed to intercept > 95% of incident radiation (Clifton-Brown et al. 2000). This was confirmed by the radiation intercepted (percentage Light Interception, LI, Figure S3), which shows there were minimal differences in the seasonal dynamics of LI between the genotypes. Based on the GLAI and LI responses from the end-season drought in 2016, the much more severe drought in 2018

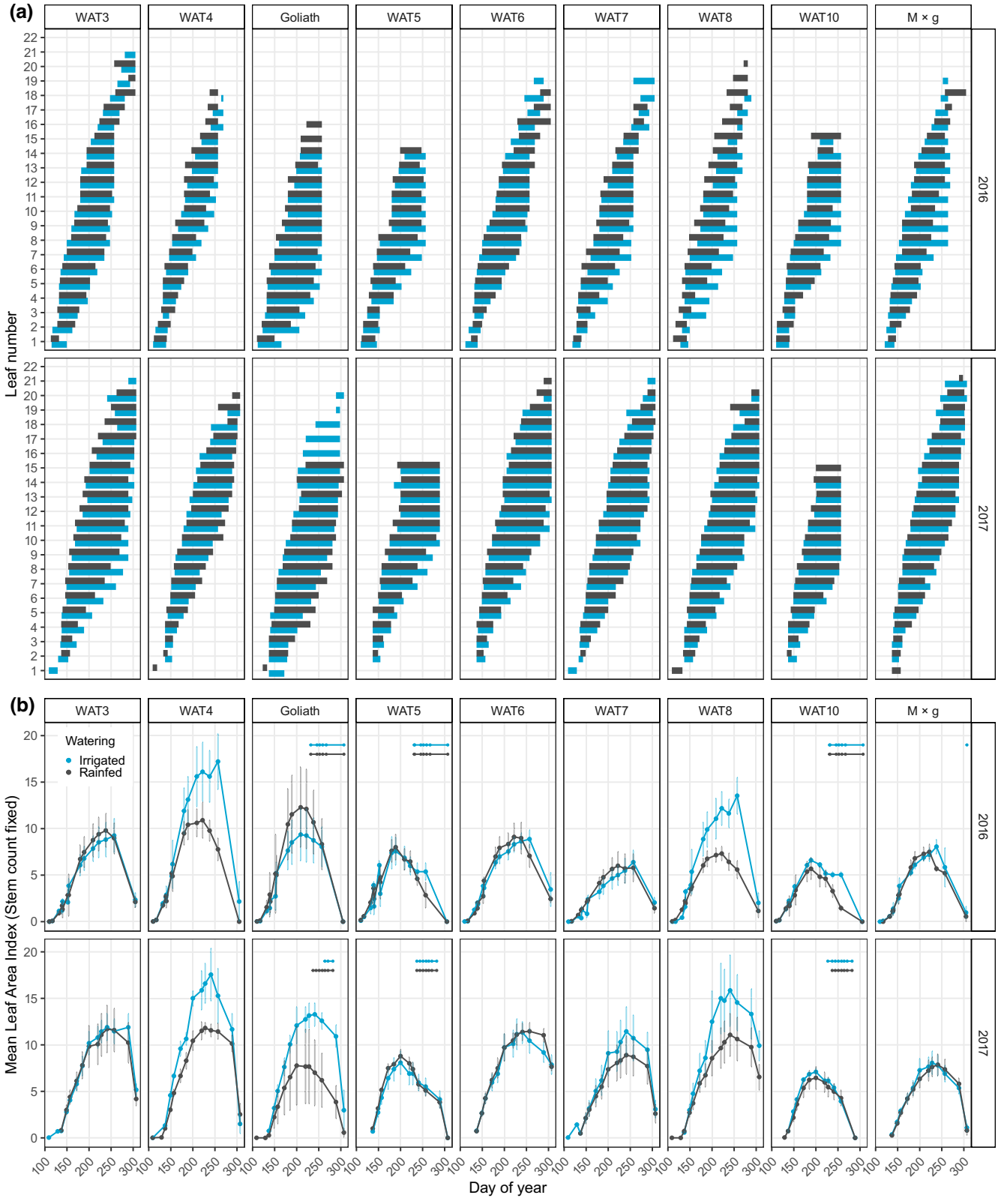

FIGURE 4 | Dynamics of the duration of individual leaves over two whole seasons: (a) Average leaf retention time over the season, showing the first and last day of the year each leaf was recorded from the bottom (leaf 1) of the plant up to the last leaf produced in the season. (b) The leaf area index as calculated from the size of the leaves. Dates for the duration of plant flowering are marked with a horizontal line at the top. Error bars ±1 SE, $n = 4$. In both (a) and (b) blue is irrigated and black is rainfed plots, leaves were only measured for two of the three trial years.

must have drastically reduced GLAI in the rainfed treatment. Interestingly, the 2018 drought only lowered LI to ~80%, only 10% less than the irrigated treatment.

Differences between genotypic responses to drought highlighted the diverse dynamics of seasonal leaf retention strategies, particularly in leaves lower down in the canopy (Figure 4B). Goliath

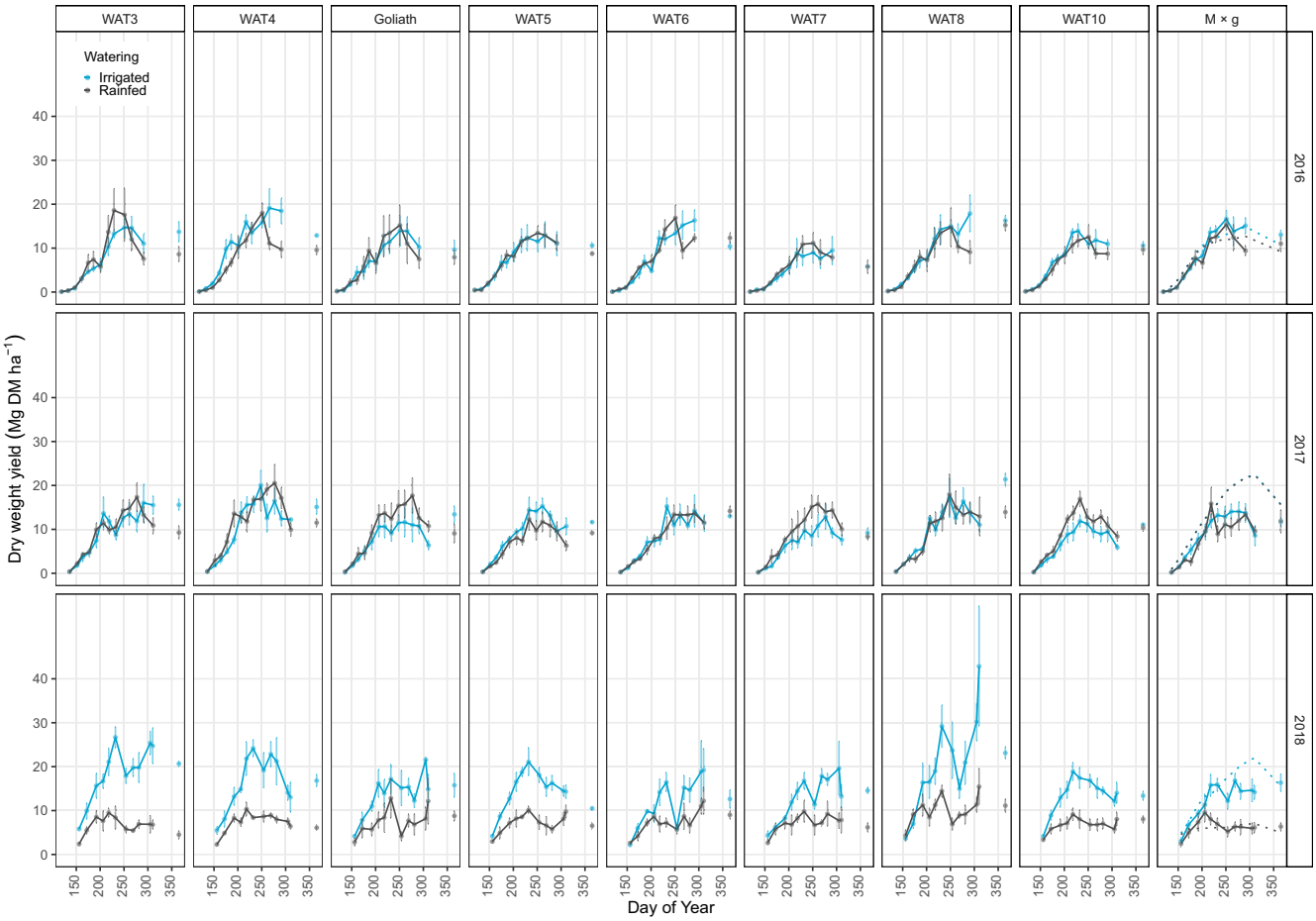

FIGURE 5 | Dynamics of above ground standing biomass (t dry matter ha-1) for nine genotypes, over three years for the WATBIO field trial located in JKI—Braunschweig, Germany. Error bars ±1 SE, $n = 4$. Unconnected dots at the end of the year show the final harvest yield in spring of the following year. Dotted lines in the $M \times g$ panels to show daily estimates of standing crop yield calculated by the model MiscanFor with and without irrigation.

and WAT3 (in the wetter year) retained green leaves longer, while $M \times g$, WAT7, and WAT4 had more leaf turnover as lower leaves were replaced by upper leaves. In response to irrigation in 2016, WAT8 and WAT4 retained the highest leaf areas during the late summer drought (Figure 4B).

The light interception from irrigated plots was higher than that in rain-fed plots in 93% of measurements. The differences were most notable in 2018 when light interception measurements from irrigated plots were on average 6% higher over the year (Figure S3). In 2016, at the end of the growing season, there is a separation in light interception as leaves are retained longer with irrigation; this is most viable in WAT4 and 8 (Figure 4A).

Estimates of the seasonal changes in the standing crop yield (scaled in Figure 5 to tonnes dry matter ha^{-1} (t DM ha^{-1})) mostly ranged from 0 to 20 t. These values were from the product of the mass of canopy contributing shoots throughout the season and their final count at the end of the growing season. There were a few genotypes in the heavily irrigated treatment in 2018 that exceeded 30 t DM ha^{-1}. In 2016 there were relatively small differences between the irrigated and rainfed plots, probably due to the late timing of the water deficits and insufficient irrigation to keep up with the evaporative demand (as shown in Figure 2 by modelling and Figure S1 by measurement). The standing crop yield dynamics showed small differences between the rainfed and irrigated treatments in 2017 but large differences in 2018. In 2018 irrigated yields were more than double the rainfed yields across all genotypes. The genotypes with the highest rainfed standing crop yields in 2018 were WAT6 and WAT8. In 2018 $M \times g$ produced not only a modest yield in the rainfed treatment but also in the irrigated treatment. Modelling parameters in the latest versions of MiscanFor include a downregulation of the RUE when temperatures are above 28°C. Including this 'overheating parameter' (based on unpublished photosynthesis measurements) ensures a good match between the modelled and observed dynamics for $M \times g$. Interestingly, when irrigated, several wild and recently bred genotypes perform better than $M \times g$ in the hot summer of 2018.

3.3 | Efficiencies for Use of Radiation and Water

The radiation use efficiency (RUE) (Figure 6) calculated by dividing the standing crop harvests (Figure 5) by the accumulative sum of the radiation interception up to each harvest date (derived from Figure S3) ranged from 0 to 3 g DM MJ^{-1} PAR.

In 2016 and 2017, the differences between the rainfed and irrigated RUEs were modest, and genotypes Goliath, $M \times g$ and

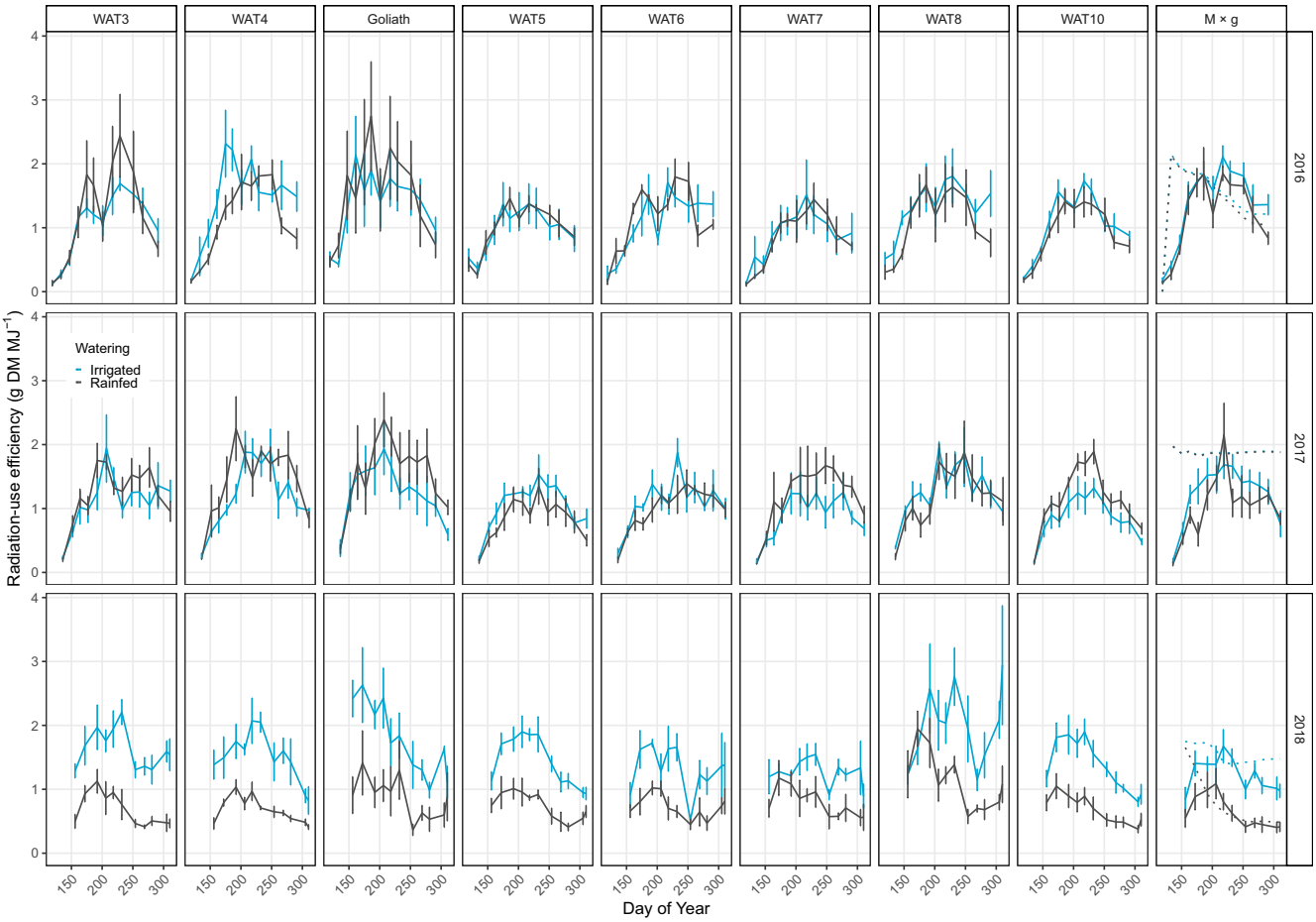

FIGURE 6 | Dynamics of cumulative radiation use efficiency for nine genotypes, over three years for the WATBIO field trial located in JKI—Braunschweig, Germany. The standard error bars (±1 SE, $n = 4$) show the variation in the biomass grown between each successive harvest. The dotted lines in the $M \times g$ panels are MiscanFor modelled estimates of the dynamics of radiation-use efficiency for irrigated and rainfed treatments.

WAT3 produced some of the highest peak RUEs. However, the pattern in the hot-dry 2018 growing season showed a strong contrast between both genotypes and the water supply treatments, with irrigation nearly doubling the RUE. At the start of 2018, RUE for WAT8 rainfed and irrigated plots was similar, but as the drought progressed, a large difference in irrigated and rainfed RUEs developed. Overall, the RUE in the rainfed WAT8 plots remained higher than all other genotypes.

The water-use efficiency (WUE) in Figure 7, calculated by dividing the cumulative mass at each successive harvest in Figure 5 by the cumulative rainfall and irrigation, ranged from 2 to 6 g DM (kg H_2O)$^{-1}$. Overall, WUEs in 2016 and in 2018 were higher than in the wet year of 2017. In 2018, when the plants were placed under prolonged and severe water deficits, there were large differences between the irrigated and rainfed treatments.

3.4 | Measured Yield and Yield Stability

The drought periods of 2016 and 2018 had large impacts on the productivity in all nine genotypes. In terms of final harvestable spring yield, the highest and lowest ranked genotypes (WAT8 and WAT7) over the three years produced an average of 16.8 and 8.3 t DM ha^{-1} y^{-1} respectively (Table 3).

Genotype, watering and year all significantly affected yields, with significant interactions between all three. Over the three study years, WAT8 produced significantly more biomass than all the other genotypes. In 2017, WAT6's yield slightly exceeded that of WAT8. WAT7 performed the worst but was not significantly lower than WAT10 and 5. There was a significant (3 Mg DM ha^{-1}) drop in average yields in 2018 without irrigation vs. the other rainfed years. On average, irrigation significantly increased yields by 4.3 Mg DM ha^{-1}. In the irrigated treatments, WAT3 ranked second, but without irrigation, its yield was severely reduced, especially in the extremely hot and dry year in 2018. When irrigated, WAT8 and WAT3 rank first and second every year. However, while WAT8 mostly retains its ranking despite losing > 50% of its yield under strong drought conditions, WAT3 drops 78% of its yield ranking into last place. WAT6 was always the least affected by drought, dropping only 29% in strong drought and was the only genotype to have a greater yield without irrigation in two of the years. While WAT3 was most affected by drought, over the three years it produced 9.2 Mg DM ha^{-1} lower yields from rainfed plots than from irrigated plots. $M \times g$ ranked between three and six out of nine across the treatments and years. Under either irrigated or rainfed treatments, $M \times g$, WAT6 and WAT10 do not yield as highly as WAT8.

The first of the three drought indices shown in Table 3 was the first developed; the drought stress tolerance index is designed to

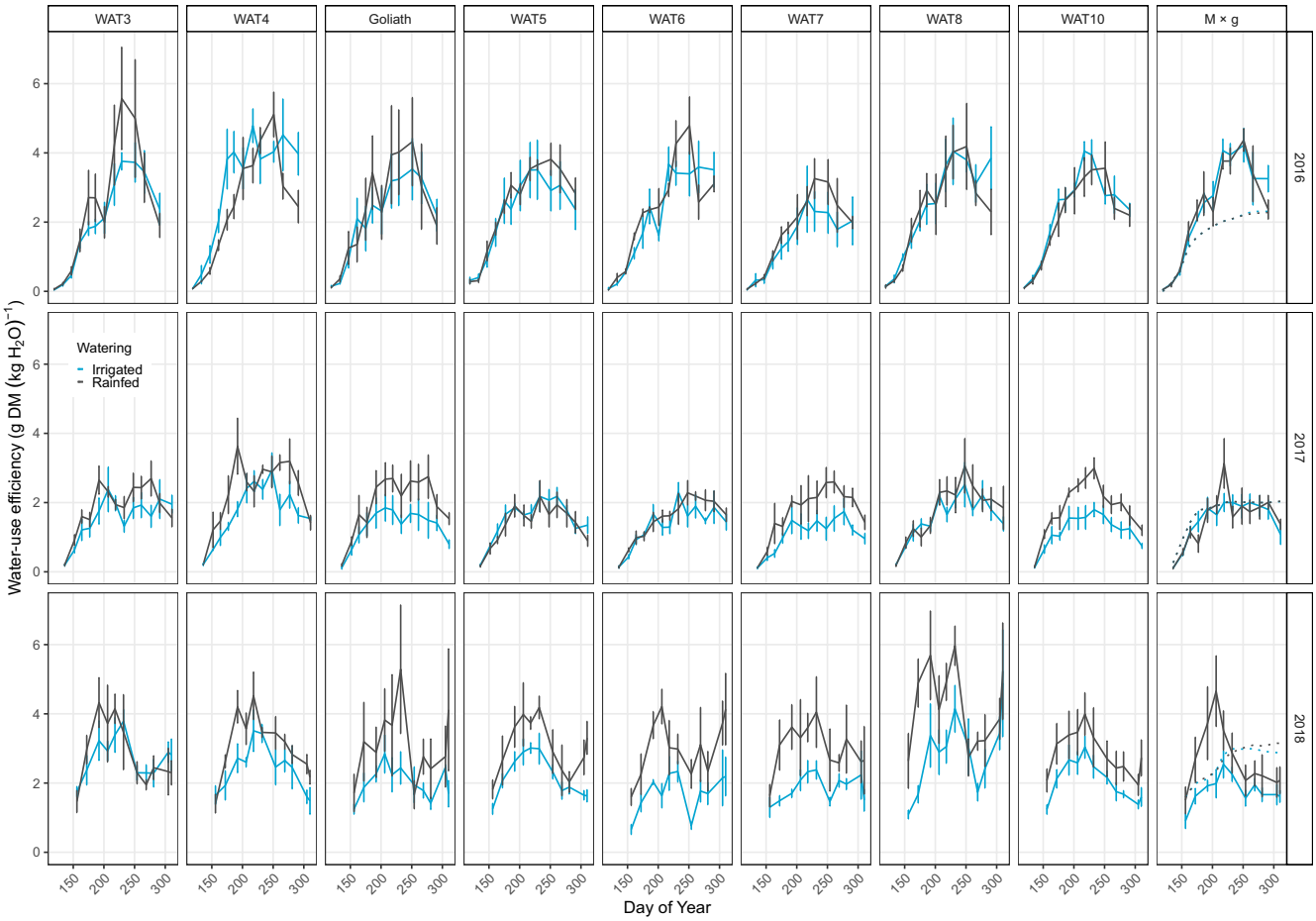

FIGURE 7 | Dynamics of cumulative water use efficiency (WUE) for nine genotypes, over three years for the WATBIO field trial located in JKI—Braunschweig, Germany. The standard error bars (±1 SE, $n=4$) show the variation in the biomass grown between each successive harvest. The dotted lines in the $M\times g$ panels are MiscanFor modelled estimates of the dynamics of water-use efficiency for irrigated and rainfed treatments.

measure yield stability relative to the wider population. WAT3 and WAT4 are notably poorer performing in this index, mirroring their yield loss percentage rankings. The stress tolerance index takes more account of the overall yield difference, not just the loss relative to other genotypes, so this ranks WAT8 best and WAT7 worst. This is despite some low percentage losses; for example, in 2016 WAT7 dropped 1% while WAT8 dropped 6% of its yield under drought, but WAT8's yield was 3× that of WAT7, thereby producing a higher rank. Lastly, the yield stress score is an average of the stress tolerance index and stress susceptibility and aims to combine both approaches but tends to more reflect stress susceptibility. This combination metric highlights the differences between WAT6 and WAT8.

3.5 | Modelled Yields

MiscanFor was run using existing parameters developed from $M\times g$ for the site. The modelled predictions matched the observed rain-fed and irrigated yields for the three years as shown in Figure 1 with an $R^2=0.95$. Parameters were changed for WAT6 to establish a model yield match to experimental data with $R^2=0.97$. This involved an earlier shooting start to 100 degree days base 1 (DD_1), a higher threshold for LAI expansion and RUE of 1500 kPa soil capillary pressure and increasing the threshold of overheating to 35°C. For WAT8, a match of measured and modelled data ($R^2=0.967$) was achieved by using similar parameters to WAT6 with a reduced RUE max of $1.85\,g\,MJ^{-1}\,m^{-2}$ and by downregulating the RUE above 35°C by $0.16\,g\,MJ^{-1}\,m^{-2}$ for every °C rise in temperature. Using all three parameterised genotype-specific models ($M\times g$, WAT6 and WAT8), the yield was estimated for each year over the period of 2012–2022 using the Braunschweig meteorological conditions with no irrigation. Cumulative modelled yield totals show that WAT6 accumulates higher yield than WAT8, but both are larger than $M\times g$ (Figure 8).

4 | Discussion

4.1 | Breeding Miscanthus

Miscanthus is at an early stage of domestication compared to other members of the saccharum complex, and consequently, the emphasis between 2006 and 2008 was placed on the collection and characterisation of accessions from the wild in Asia (Huang et al. 2019). In situ and ex situ phenotypic selections were the first step in the breeding process (Clifton-Brown et al. 2019). As mentioned above, the standard genotype used commercially in Europe and as a control here is a triploid interspecies hybrid *Miscanthus*×*giganteus* ($M\times g$) (Greef and Deuter 1993). In addition to the potential problems

TABLE 3 | Yields determined from the final spring quadrat harvest comparing the rainfed and irrigated treatments (Mg DM ha^{-1} (±1 SE, $n=4$)).

	Year	Yield (Irrigated) ($Mg ha^{-1}$)	Ranking	Yield (rainfed) ($Mg ha^{-1}$)	Ranking	Drought change (%)	Ranking	Stress tolerance index	Stress susceptibility index	Yield stress score index
WAT3	2016	13.72 ± 2.3	2	8.62 ± 1.7	7	−37	1	0.9	2.7	1.8
	2017	15.57 ± 1.2	2	9.27 ± 1.4	6	−40	1	0.8	2.0	1.4
	2018	20.67 ± 0.6	2	4.51 ± 0.9	9	−78	1	0.4	1.5	0.9
	Total	49.97 ± 3.1	**2**	22.4 ± 3.9	**8**	−55	**1**	0.7	1.8	1.2
WAT4	2016	12.89 ± 0.3	4	9.57 ± 1.1	5	−26	2	0.9	1.9	1.4
	2017	15.11 ± 1.7	3	11.53 ± 0.9	4	−24	4	0.9	1.2	1.1
	2018	16.8 ± 1.3	3	6.1 ± 0.6	8	−64	2	0.4	1.2	0.8
	Total	44.81 ± 3.1	**3**	27.19 ± 2.5	**5**	−39	**2**	0.7	1.3	1.0
Goliath	2016	9.64 ± 2.2	8	7.93 ± 1.6	8	−18	3	0.6	1.3	0.9
	2017	13.41 ± 1.8	4	9.08 ± 2.2	8	−32	3	0.7	1.6	1.1
	2018	15.77 ± 2.7	5	8.79 ± 1.2	3	−44	6	0.5	0.8	0.7
	Total	38.82 ± 6.3	**5**	25.81 ± 4.0	**6**	−34	**4**	0.6	1.1	0.8
WAT5	2016	10.62 ± 0.6	5	8.76 ± 0.5	6	−17	4	0.7	1.3	1.0
	2017	11.65 ± 0.2	7	9.16 ± 0.5	7	−21	5	0.6	1.1	0.8
	2018	10.51 ± 0.4	9	6.54 ± 0.7	5	−38	8	0.3	0.7	0.5
	Total	32.78 ± 1.0	**8**	24.47 ± 1.5	**7**	−25	**7**	0.5	0.8	0.6
WAT6	2016	10.4 ± 0.8	7	12.33 ± 1.1	2	19	9	1.0	−1.3	−0.2
	2017	13.0 ± 0.2	5	14.17 ± 1.1	1	9	9	1.0	−0.5	0.3
	2018	12.63 ± 2.1	8	9.02 ± 0.9	2	−29	9	0.4	0.5	0.5
	Total	36.04 ± 2.9	**6**	35.53 ± 3.0	**2**	- 1	**9**	0.8	0.0	0.4
WAT7	2016	5.82 ± 0.5	9	5.77 ± 1.5	9	- 1	8	0.3	0.1	0.2
	2017	9.2 ± 1.1	9	8.36 ± 0.8	9	- 9	6	0.4	0.5	0.4
	2018	14.55 ± 0.7	6	6.18 ± 1.0	7	−57	4	0.4	1.1	0.7
	Total	29.57 ± 2.1	**9**	20.31 ± 3.1	**9**	−31	**5**	0.4	1.0	0.7

(Continues)

TABLE 3 | (Continued)

	Year	Yield (Irrigated) (Mg ha^{-1})	Ranking	Yield (rainfed) (Mg ha^{-1})	Ranking	Drought change (%)	Ranking	Stress tolerance index	Stress susceptibility index	Yield stress score index
WAT8	2016	16.28 ± 1.2	1	15.23 ± 1.3	1	- 6	7	1.9	0.5	1.2
	2017	21.39 ± 1.4	1	13.91 ± 1.3	2	−35	2	1.6	1.8	1.7
	2018	23.12 ± 1.4	1	11.12 ± 1.5	1	−52	5	1.0	1.0	1.0
	Total	60.78 ± 3.5	**1**	40.26 ± 3.4	**1**	−34	**3**	1.5	1.1	1.3
WAT10	2016	10.6 ± 0.8	6	9.67 ± 1.1	4	- 9	6	0.8	0.6	0.7
	2017	11.05 ± 0.5	8	10.39 ± 0.8	5	- 6	7	0.6	0.3	0.5
	2018	13.37 ± 1.0	7	8.04 ± 0.8	4	−40	7	0.4	0.7	0.6
	Total	35.03 ± 1.6	**7**	28.1 ± 2.6	**4**	−20	**8**	0.6	0.6	0.6
M×*g*	2016	13.07 ± 1.0	3	11.02 ± 1.7	3	−16	5	1.1	1.1	1.1
	2017	11.7 ± 1.0	6	11.9 ± 2.6	3	2	8	0.8	−0.1	0.3
	2018	16.34 ± 2.0	4	6.36 ± 0.9	6	−61	3	0.4	1.1	0.8
	Total	41.11 ± 3.6	**4**	29.27 ± 4.0	**3**	−29	**6**	0.7	0.9	0.8

Note: Within year and average across all year rankings for different genotypes within irrigated and rainfed treatments are shown (Ranking irrigated and rainfed) (blue is high yield, red is low yield) and between the treatments (drought change percent, and ranking) (blue is low change, red is high change). Yield stability indices were calculated with the equations in Table 2 (blue is stable, red is unstable). (editable .xlsx uploaded separately).

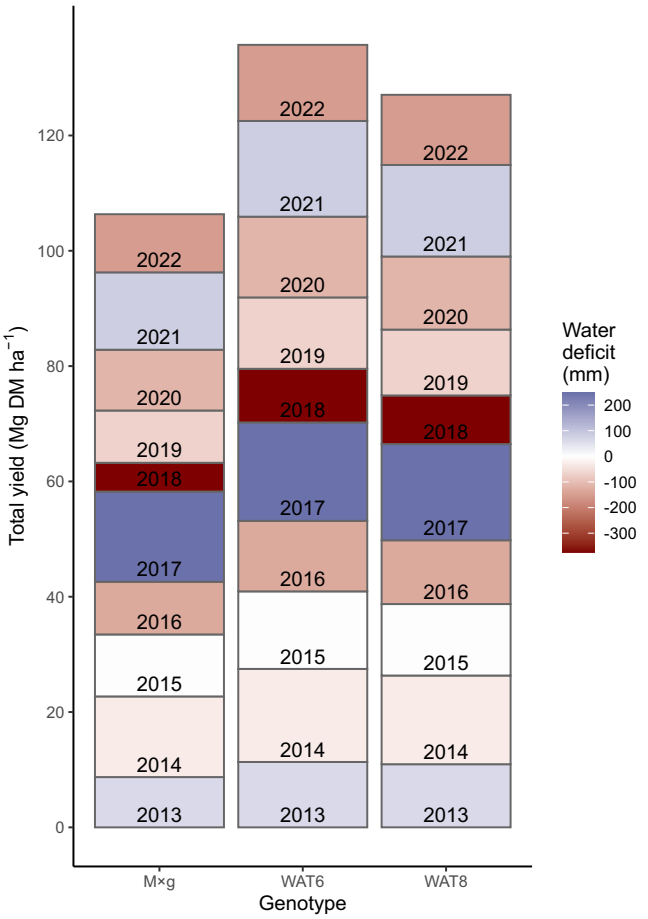

FIGURE 8 | Modelled yields for three genotypes accumulated over 10 years around the 3 year trial period. Colours show modelled evapotranspiration minus precipitation from −373 in 2018 (deep red) to +247 in 2017 (dark blue).

associated with large-scale adoption of a single or small number of clones, such as disease pressure, there are other potential problems with $M \times g$. A significant one is that studies have demonstrated that the yield of $M \times g$ is particularly vulnerable to water deficits (Malinowska et al. 2017); (Clifton-Brown and Lewandowski 2000). Therefore, it is necessary to broaden the available commercial *Miscanthus* genotypes. Ideally, this should be done over a short period to have the maximum impact on aims to decarbonise economies and impact on the trajectory of climate change. To achieve rapid improvements over short periods of time, we previously tested several breeding strategies and demonstrated the superior yields achieved from hybrids when compared to, for example, the fastest approach of directly exploiting wild accessions (Clifton-Brown et al. 2019). We further hypothesised that crossing parental lines from diverse regions (so-called wide hybrids) could produce even higher yielding and more resilient hybrids than $M \times g$. The germplasm used in the trial represents the best genotypes from a pool of both accessions and hybrids from the breeding programme available at the beginning of the study.

Interspecific crosses in other crops such as wheat have resulted in impressive yield gains (Ortiz et al. 2008); however, interspecific crosses are challenging to produce and often result in sterility. Of the wild relatives collected, it has been estimated that less than 10% have been used in interspecific crosses (Reynolds and Langridge 2016). There appears to be few, if any, genetic barriers to generating crosses between diverse Miscanthus (Figure 4, Clifton-Brown et al. 2019). Additionally, because Miscanthus is a relatively new crop, other problems associated with the use of wild germplasm, such as linkage drag (Zhang et al. 2025), are less of an issue. We therefore generated and selected from a large population of Miscanthus accessions and hybrids to examine field responses to variation in water availability.

The source of genotype WAT4 (*M. sacchariflorus* robustus type) is a highly saline environment and therefore a good candidate for resilience traits. In particular, the initial stages of salt stress, before ion toxicity, resemble drought stress (Munns et al. 1995). Previously, the converse approach was demonstrated when *Miscanthus* selected for drought stress were compared under saline stress (Stavridou et al. 2019). The robustus genotype, WAT4, responded to drought through large reductions in yield. Along with WAT3, WAT4 ranked mostly among the two plants where yield declined the most in response to drought and, as a partial consequence, ranked poorly in all drought indices. Five genotypes chosen for the study (WAT3, 4, 9 ($M \times g$), 10 and Goliath) are in common with a previous pot experiment in which different physiological parameters, including photosynthesis and stomatal responses, were measured (Malinowska et al. 2020). WAT3 was the most impacted genotype in the field and pot experiments and had the second highest level of phenotypic plasticity in the pot experiments after $M \times g$ when several traits, including stem, biomass and stomatal responses, were combined (Malinowska et al. 2020). Genotype WAT10 had the lowest phenotypic plasticity in response to drought, which is consistent with its high rankings in the stress susceptibility and yield stress scores (Table 3). In the pot experiments, $M \times g$ had the highest values for stomatal conductance; highest plasticity, and it was concluded that this genotype displayed an "optimistic" growth habit. This is consistent with water extraction as measured by soil water reflectometers in the field study; however, yield in $M \times g$, while still being significantly impacted by drought, was more stable than expected in terms of stress indices. This may reflect that the field studies reported here span the whole season, whereas pot studies are shorter and thus do not allow counterfactuals such as potential adjustments in seasonal growth duration to reduce the impact of water stress on yield. In contrast to the optimistic genotypes, others, such as WAT5, tended to conserve water and have low yields even when water was available. This strategy may be considered classically as stress tolerance but does not appear well-suited to biomass crops in both this study and other studies of drought in Miscanthus (Malinowska et al. 2020) or in other crops such as maize where high performance under favourable conditions was linked to high performance under drought (Djemel et al. 2019). One of the best genotypes for yield in all conditions (WAT8) grew rapidly while water was available but reduced growth and transpiration rates in unfavourable conditions but resumed growth when rainfall returned. Whether new growth comes from new shoots or existing stems depends on leaf retention, which seems to vary greatly with genotype (e.g., WAT7 vs. Goliath). Goliath (WAT11) is an example of *M. sinensis* . Several papers report that *M. sinensis* has a higher tolerance to drought than

M. sacchariflorus (Malinowska et al. 2017; Weng et al. 2021). Indeed, *M. sacchariflorus* is generally found near water; both fresh and saline (Dwiyanti et al. 2013). Within *M. sacchariflorus* , there is a wide genetic diversity, with tall *M. sacchariflorous* spp. Lutariorparius indigenous to central China (Xi and Jezowkski 2004) and a much shorter *M. sacchariflorus* indigenous to Northern China and Southern Russia (Clark et al. 2019). Collections of the shorter *M. sacchariflorus* , for ornamental purposes, were brought to St. Petersberg in 1855/6 by Carl Maimowicz and were found to be winter-hardy there and were named 'Robustus' (Clark et al. 2019). When interspecies crosses between *M. sinensis* and *M. sacchariflorus* 'Robustus' are made, some progeny are both higher yielding and more stress resilient than their parents (pers. comm. European Miscanthus breeders: Martin Deuter, Kai-Uwe Schwarz and John Clifton-Brown). WAT6 and WAT8's superior performance could be attributed to a similar form of wide cross heterosis, but the nature of such genomic interactions is unknown (Xi and Jezowkski 2004; Dwiyanti et al. 2013; Clark et al. 2019). The question remains, given the selection of accessions and the breeding of diverse hybrids in Miscanthus, how best to identify improved Miscanthus for rapid deployment.

Large scale breeding efforts for crops that have been developed for decades can utilise data from many years and many sites in a meta-analysis to identify elite germplasm and or hybrids (e.g., Semagn et al. 2013). However, Miscanthus is a relatively new crop with fewer data from diverse field sites to draw upon. It is therefore in some ways a simpler proposition in terms of generating diverse hybrids but a more challenging one in terms of assessing the potential impacts of new hybrids. Modelling of yield is one approach to provide additional information regarding yield over years that are not empirically determined. Also, modelling has been discussed in the context of breeding programmes, for example to aid in ideotype design (Rötter et al. 2015) or to aid decision making in breeding programmes (Sun et al. 2011). The use of modelling may be particularly important in a crop such as Miscanthus in which a single plantation can be grown and harvested for more than 20 years (2020).

4.2 | Modelling *Miscanthus* Growth

Modelling may provide a level of assurance of the relative performance of different Miscanthus genotypes across multiple environments (years) at the same (or similar) site(s) and of potential impacts from future climate scenarios. It is also a general aim in Miscanthus cultivation to use minimal agronomy for a superior energy balance and high levels of sustainability, and this is being enshrined in some legislation regarding the use of biomass for certain products (e.g., RED II, Webster 2020). Consequently, agronomy that could be used to help improve yield in challenging years may not be routinely deployed in such crops. It has been argued that to best utilise simulation modelling in crop development one main goal is to obtain a 'better understanding of plant processes that limit productivity under future climate change' (Ramirez-Villegas et al. 2015). Many such studies are focused on grain crops, but biomass crop growth is highly sensitive to water availability (Price et al. 2004; Kørup et al. 2018; Coelho et al. 2019). Here we utilised a field trial on free draining soil to generate contrasting water environments from irrigated and rain-fed plots. In addition, the trial was especially fortunate in encompassing three years in which meteorological conditions were very diverse (Figure 3). The year 2018 was one of the hottest and driest summers over Northern Europe (Peters et al. 2020) with negative impacts on the yields of spring sown crops. In stark contrast, 2017 was an unusually wet year with an even rainfall pattern throughout the growing season. These large annual contrasts in water availability between 2016, 2017 and 2018 during our experiment with the contrast between the irrigated and rainfed treatments combined to make a particularly useful dataset for quantifying the impacts of weather extremes on growth dynamics and the final biomass yield under future climates. The extensive phenology and physical measurements enable the drivers of difference in the observed measurements to be mimicked by changing the model parameters. This enabled the determination that WAT6 was less sensitive to both overheating and water deficit than $M \times g$ and that WAT8 was sensitive to water deficit but not overheating. However, although WAT6 was relatively insensitive to the environment it has a lower biomass accumulation rate, WAT8, on the other hand, outperformed $M \times g$ in well-watered and drought conditions. The sensitivity of WAT8 to water deficit meant that overall, due to large interannual variations in yield due to meteorological conditions, it was predicted to underperform WAT6 over the 10-year modelled period (Figure 9).

4.3 | Dynamics of Growth Traits

The fortnightly measurements of above-ground traits, including height, flowering time, leaf development (LAI) and light interception (LI), showed many differences between irrigated and rainfed treatments for the different genotypes. Smaller variations were observed in the start of the growing season (emergence time of the shoots from the overwintering rhizome) in these genotypes than in more recent trials planted in 2018 (Magenau et al. 2023). However, there was a significant difference between the height of different genotypes by 1 July (before any flowering occurs), showing differences in the rate of growth (Figure 3). Light interception differences were less than expected between the genotypes but were highly significant between the rainfed and irrigated treatments (Figure S3). The dynamics of the above-standing biomass derived from the fortnightly dry weights of sampled shoots also showed large differences. In this trial, we measured these by the regular harvests (known as 'serial cuts') of randomly selected shoots contributing to the canopy. When these weights are multiplied by the shoot counts per m^2 the dynamics of yield can be plotted, but there is a high risk of overestimation of yield due to the counting of shoots that are no longer contributing to the canopy. Our solution to stabilizing the in-season yield growth curves was to relate the final serial cut to the final quadrat harvested yields. This avoids the need to use shoot counts in the yield estimation. The accuracy and precision are both improved sufficiently to calculate the RUE and when these are combined with the non-destructive phenotyping measurements, where repeated measures are possible, robust parameters for key processes such as the start of growth, rates and brakes during the growing period were

derived—including the impacts of water deficits if these occur and the triggers for the end of growth. The leaf area dynamics recorded in 2016 and 2017 for all the leaves on marked stems show the dynamics of senescence. Interestingly, in 2016, senescence during the water deficit in August had little detectable impact on the percentage of the light intercepted by the canopy. That is to be expected because leaf area indices > 4 can intercept incident light with efficiencies above 90%. Unfortunately, the detailed measurements of the leaf dynamics were not continued in 2018 when the severe prolonged drought would have shown the greatest differences between the genotypes. However, as with the drought in 2016, the impacts on light interception (Figure S3), though detectable, were quite small in all genotypes except WAT3, which reduced its leaf area, reducing transpiration and leaving more water in the soil profile than $M\times g$ and WAT10. These differences in water extraction warrant further research due to their wider hydrological impacts.

The strong contrasts in the climatic conditions between the three successive growing seasons were quantified in terms of soil capillary pressure in the soil and vapour pressure in the atmosphere. In the soil, the unreplicated measurements of volumetric soil moisture content with the reflectometers under three genotypes at two depths (Figure S1) concurred well with the modelled seasonal patterns. During the dry periods of 2016 and 2018, the soil reflectometers also gave a further insight into the rates of drying in the soil profile. With full canopy closure (from June onwards), $M\times g$ uses the available water rapidly, while *M. sinensis* (Goliath) dries the soil more slowly. Although to some extent this observation is anecdotal, because we did not have the resources to instrument the four replicates, it does concur with earlier pot experiments, where it was observed that mature $M\times g$ grows fast and transpires fast. Irrigation levels at close to 80 ETo, particularly in the prolonged drought of 2018 on $M\times g$, had huge effects on growth rates (Figures 3 and 5). This brings us to an important question: are the genotypes with the highest yield potential always going to have lower yield stability? And based on the yield data in Figure 7 the answer is probably yes, most of the time. However, the genotype WAT8 that was also high yielding showed a higher yield stability than $M\times g$—when comparing the two treatments within a drought year and when comparing between the different years. The genotypes that can break this general rule are particularly interesting for genetic improvement programmes.

In this study, leaf area, light interception and standing yield (estimated during the growing season) had large observed differences between growing seasons, but smaller yet significant differences between the genotypes. Differences in drought response can also be due to phenological stage (Daryanto et al.

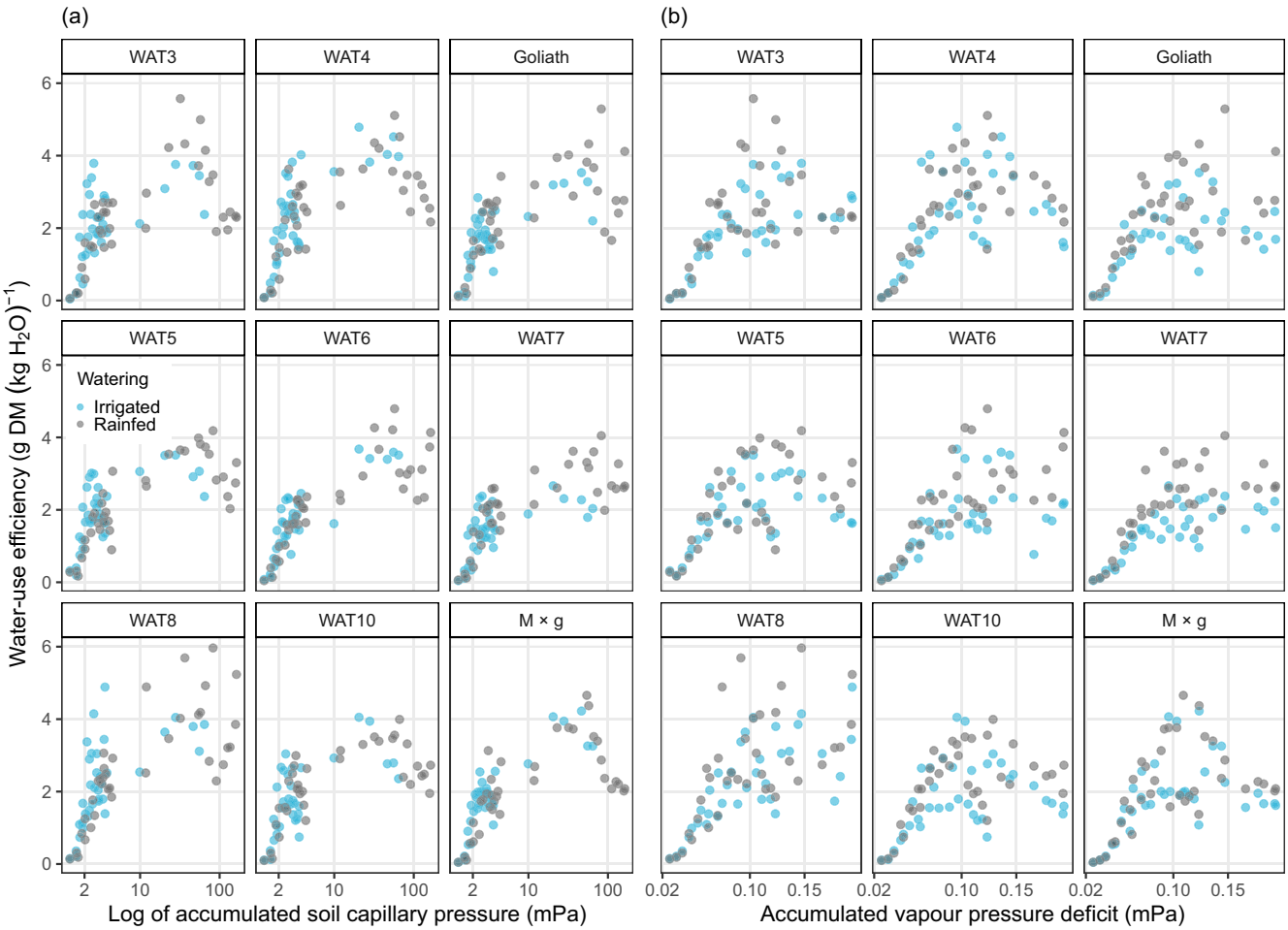

FIGURE 9 | Cumulative water use efficiency estimated from measurements of standing crop yield across all three years for each genotype plotted against soil capillary pressure estimated by MiscanFor from the Plant available water (PAW, 150 mm) (a) and Vapour pressure deficit (VPD) averaged from the 9 am daily measurements of humidity and temperature (b). Blue dots are irrigated, and Black dots are rainfed.

2017), so genotypes like WAT8 could grow quickly to catch up after the drought. While at the other extreme, genotypes that flowered early avoided growth during the height of the drought but remained small.

4.4 | Dynamics of RUE and WUE

The quantity of the intercepted radiation that was converted into aboveground biomass varied was used to derive the key modelling parameter 'radiation use efficiency' (RUE). Average overall RUE calculated with the accumulative intercepted radiation varied from 0.1 to 3.0 g DM MJ^{-1}, similar to those values reported from cooler sites (Van der Werf et al. 1993; Clifton-Brown et al. 2000; Davey et al. 2017). As the green leaf area remained high enough to capture > 80% of the light from June to September, the differences between the genotypes' biomass growth during the mid and late season deficits must lie more in the impacts of the water deficits on the efficiency of light conversion (RUE) rather than capture (Light interception %).

One possible explanation could be that on this sandy site in Braunschweig, even in the irrigation treatment, RUEs were reduced by water deficits. This limitation is seen in 2016 in the modelled capillary pressure, but not in the irrigated treatment in 2018, when it appears that the higher irrigation rates were sufficient to cover evaporative demand (Figure 3). However, the measurements of volumetric soil moisture content at 25 and 75 cm in Figure S1 show that the minimum soil moisture contents in irrigated plots were in the range 6%–7%. Although intensive physiological measurements were not performed in this trial (as in other trials, e.g., Beale et al. 1996), a pre-dawn plant water potential during the drought period would no doubt confirm that the tensions were well below the traditional wilt point of −1.5 MPa, and this could well explain the lower than expected RUE.

4.5 | Physiological Breeding for Improved Biomass and Water Use Efficiency

WUE is discussed as an essential component in reducing the impacts of agriculture and increasing its resilience to climate change (Hoover et al. 2023). Mechanistically, this is more complex and Blum (2009) for example, argues that selecting for WUE will intrinsically select for traits that decrease water use and these traits usually also decrease biomass accumulation. However, WUE may be of particular importance for long-season crops, such as Miscanthus, where growth may pass through many phases of water availability and either conserving water or the optimal use of water to fix carbon may be considered paramount to maximize biomass accumulation over the season. The values of WUE calculated in our experiments for above-ground biomass ranged from 2 to 6 g DM (kg $H_2O)^{-1}$ under extreme drought, agreeing well with an earlier controlled environment pot experiment (Clifton-Brown and Lewandowski 2000). In a field experiment, Beale et al. (1999) estimated the WUE of above-ground biomass for rainfed Miscanthus ($M\times g$) to be 9.1 g DM (kg H_2O). The MiscanFor model calculates losses of both runoff and drainage through the profile. Even when these losses are subtracted in the WUE calculation, our estimates for $M\times g$ are considerably lower than those of Beale, whose high values have been seen in container experiments (Malinowska et al. 2017) but not in the field.

To explore further the physiological differences associated with WUE dynamics, the capillary pressure (which determines the supply (or push) of water from the soil to the plant) and the atmospheric vapour pressure deficits (or pull) were visualised (Figure 9). As expected, there was an overall positive correlation between soil capillary pressure and WUE. At low capillary pressures, WUEs averaged about 2 g DM (kg $H_2O)^{-1}$. At higher capillary pressure, the WUEs ranged between 4 and 6 g DM (kg $H_2O)^{-1}$. Notably, at low capillary pressure, WAT3, 4 and 8 produced WUEs up to 5 g DM (kg $H_2O)^{-1}$, which contribute to their higher overall WUE. Interestingly, we note different response profiles when comparing $M\times g$ and the higher yielding genotypes WAT6 and WAT8. $M\times g$ has a bell-shaped response, with WUE declining under the more extreme drought occurrences, whereas WUE values in WAT8 under the same extremes were more variable but higher and lacking the pronounced decline seen in data from $M\times g$. The more conservative genotypes, such as WAT5, appear to achieve an early asymptotic relationship between WUE and soil capillary pressure and a bell-shaped response to VPD, albeit achieving slightly lower maximum values of WUE than WAT8.

The bell-shaped curve seen relating soil capillary pressure and WUE in $M\times g$ represents an expected biphasic response. In the first phase under lower soil capillary pressures, it is expected that the plant responds by largely reducing water use while sustaining some level of biomass production; in the second phase, the more extreme drought conditions result in continued loss of water but no further carbon fixation, and therefore WUE declines. This is seen at the ecosystem and plant levels. Of interest are plants that can sustain production at high WUE. WAT8 is the best example of such a genotype from our study. The exact mechanism cannot be known at this time, but for example, soil hydraulic conductivity, or relative permeability of water in a partially air-filled porous medium, has been proposed to be the primary driver of stomatal closure (Carminati and Javaux 2020), so perhaps WAT8 either maintains access to more water in the soil by deep or finer roots or conserves the water that is available by a more conservative use and thus keeps stomata functioning longer for photosynthetic gas exchange. The control of water use efficiency and associated biomass accumulation is complex, and many physiological parameters could be measured that were not part of this study. The physiological mechanisms underpinning the superior performance of WAT6 and WAT8 need further investigation to separate above-ground transpiration control mechanisms such as dynamic stomatal control to evaporative demand (VPD) and thermal responses of net CO_2 assimilation (photosynthesis vs. respiration) and the below-ground processes such as increasing root depth and hydraulic conductivity of roots through processes such as osmoregulation.

5 | Conclusions

Two recently bred interspecies Miscanthus hybrids (WAT6 and WAT8) produced more biomass than standard *Miscanthus* × *giganteus* ($M\times g$) in an irrigated versus rainfed field trial on

light soil in Braunschweig, Germany, over three consecutive and highly contrasting years (2016–18). Seasonal dynamics of leaf canopy development, radiation use efficiency (RUE) and water use efficiency (WUE) were derived from sequential measurements and used to generate genotype-specific parameters in the biomass model MiscanFor. Interpolations of RUE and WUE associated with simulations of soil water supply in the irrigated and rainfed treatments and the atmospheric water demand were used to explore genotype-specific response strategies to water deficits. There was a genotypic effect on the dynamics of variation in WUE in response to drought, with new hybrids able to sustain higher values of WUE, whereas WUE declined rapidly at more extreme drought values in $M \times g$. The adjustments to parameters for model simulations of WAT6 and WAT8 suggest changes in RUE and thermal limitations may be important in these genotypes. The improved models can be used for better predictions of spatial and temporal variation in biomass yield levels and yield stability for future climate scenarios. WAT8 displayed higher efficiencies in the drought year 2018 than all other genotypes, including the standard $M \times g$, but overall WAT6 has the most consistent yield, and if modelled as rainfed over the 10 years, it is superior to WAT8. Genetic improvement through wide crossing of diverse wild-sourced ecotypes of *M. sacchariflorus* and *M. sinensis* has immense potential to produce hybrids that are both high yielding and resilient, suitable for biomass production in current and future central European climates.

Author Contributions

Danny Awty-Carroll: data curation, formal analysis, investigation, methodology, software, visualization, writing – original draft, writing – review and editing. **Paul R. H. Robson:** conceptualization, data curation, formal analysis, funding acquisition, investigation, methodology, project administration, resources, software, supervision, validation, visualization, writing – original draft, writing – review and editing. **Kai-Uwe Schwarz:** conceptualization, data curation, funding acquisition, investigation, methodology, resources, supervision, validation. **Heike Meyer:** data curation, methodology. **Jörg Michael Greef:** project administration, resources, supervision. **Astley Hastings:** formal analysis, investigation, methodology, software, writing – review and editing. **John Clifton-Brown:** conceptualization, data curation, investigation, methodology, supervision, writing – original draft, writing – review and editing.

Acknowledgements

This work was initiated as part of the project WATBIO (Development of improved perennial non-food biomass and bioproduct crops for water-stressed environments, 311922) building OPTIMISC (Optimizing Miscanthus Biomass Production, 289159), which were both supported by the European Union's Seventh Programme. Danny Awty-Carrol was supported by the BBSRC through the GIANT-LINK (LK0863), MUST (BB/N016149/1) and OMENZ (TER-303-1-M) projects. Paul Robson was supported by EU WATBIO and the UK Biotechnology and Biological Sciences Research Council's Strategic Programme for Resilient Crops (grants BB/K01711X/1, BBS/E/IB/230001C, BB/CSP1730/1). Kai Schwarz, Heike Meyer and Jörg Greef were supported by WATBIO, Fachagentur Nachwachsende Rohstoffe (FNR), Bundesministerium für Ernährung und Landwirtschaft (Züchtung neuer samenvermehrter Miscanthus-Hybriden, 22016016) and the Julius Kühn-Institute. Astley Hastings was funded by the UKRI PCB4GGR (BB/V011553/1) and UKERC-4 projects. John Clifton-Brown was supported by OPTIMISC, WATBIO, GIANT, MUST and FNR projects and during the write-up phase in 2025 by the European Innovation Partnership for Productivity and Sustainability in Agriculture (EIP-Agri) project: Integration of perennial Miscanthus strips on arable land, Regierungspräsidium Gießen, Project number 9100447-Invest-1. The authors would like to express thanks to Gail Taylor (UC Davis), Iain Donnison (IBERS) and Donal Murphy-Bokern (Lohne, Germany) for setting up and coordinating WATBIO; Chris Ashman for setting up the soil moisture reflectometers; and Heidi Strauch for field work assistance; Dr. Frank Höppner for supplying the JKI daily weather data; Chris Glover for providing information on the breeding; Umut Kirdemir for helpful discussions on the statistical analysis of the yield. Finally, J.C.-B. would like to acknowledge that the Miscanthus modelling to 'guide breeding' was started by a collaboration between my PhD supervisor Mike Jones (Trinity College Dublin) and his friend, the late Steve Long (founder of GCB), who died on the 9th September 2025.

Conflicts of Interest

The authors declare no conflicts of interest.

Data Availability Statement

The data that support the findings of this study are openly available at DOI 10.17605/OSF.IO/63EXH.

References

Allen, R. G., L. S. Pereira, D. Raes, and M. Smith. 1998. *Crop Evapotranspiration—Guidelines for Computing Crop Water Requirements—FAO Irrigation and Drainage Paper 56*. Food and Agriculture Organisation.

Al-Salman, Y., F. J. Cano, E. Mace, D. Jordan, M. Groszmann, and O. Ghannoum. 2024. "High Water Use Efficiency due to Maintenance of Photosynthetic Capacity in Sorghum Under Water Stress." *Journal of Experimental Botany* 75, no. 21: 6778–6795.

Awty-Carroll, D., A. Iurato, D. Scordia, et al. 2024. "Achieving Hybridisation Between Miscanthus Species: Commercially-Scalable Methods to Manipulate Flowering Synchronisation and Maximise Seed Yield." *Industrial Crops and Products* 219: 119116.

Beale, C. V., D. A. Bint, and S. P. Long. 1996. "Leaf Photosynthesis in the C4-Grass *Miscanthus* × *giganteus*, Growing in the Cool Temperate Climate of Southern England." *Journal of Experimental Botany* 47: 267–273.

Beale, C. V., J. I. L. Morison, and S. P. Long. 1999. "Water Use Efficiency of C4 Perennial Grasses in a Temperate Climate." *Agricultural and Forest Meteorology* 96, no. 1–3: 103–115.

Blum, A. 2009. "Effective Use of Water (EUW) and Not Water-Use Efficiency (WUE) is the Target of Crop Yield Improvement Under Drought Stress." *Field Crops Research* 112, no. 2–3: 119–123.

Campbell, G. S. 1985. *Soil Physics With BASIC: Transport Models for Soil-Plant Systems*. Vol. 14. Elsevier.

Carminati, A., and M. Javaux. 2020. "Soil Rather Than Xylem Vulnerability Controls Stomatal Response to Drought." *Trends in Plant Science* 25, no. 9: 868–880.

Clark, L. V., X. Jin, K. K. Petersen, et al. 2019. "Population Structure of *Miscanthus sacchariflorus* Reveals Two Major Polyploidization Events, Tetraploid-Mediated Unidirectional Introgression From Diploid M. Sinensis, and Diversity Centred Around the Yellow Sea." *Annals of Botany* 124, no. 4: 731–748.

Clifton-Brown, J., A. Hastings, M. Mos, et al. 2017. "Progress in Upscaling *Miscanthus* Biomass Production for the European Bio-Economy With Seed-Based Hybrids." *Global Change Biology. Bioenergy* 9, no. 1: 6–17.

Clifton-Brown, J., K.-U. Schwarz, D. Awty-Carroll, et al. 2019. "Breeding Strategies to Improve *Miscanthus* as a Sustainable Source of Biomass for Bioenergy and Biorenewable Products." *Agronomy* 9, no. 11: 673.

Clifton-Brown, J. C. 1997. *The Importance of Temperature in Controlling Leaf Growth of Miscanthus in Temperate Climates. (PhD)*. Trinity College Dublin.

Clifton-Brown, J. C., and I. Lewandowski. 2000. "Water Use Efficiency and Biomass Partitioning of Three Different *Miscanthus* Genotypes With Limited and Unlimited Water Supply." *Annals of Botany* 86: 191–200.

Clifton-Brown, J. C., I. Lewandowski, B. Andersson, et al. 2001. "Performance of 15 Miscanthus Genotypes at Five Sites in Europe." *Agronomy Journal* 93, no. 5: 1013–1019.

Clifton-Brown, J. C., B. M. Neilson, I. Lewandowski, and M. B. Jones. 2000. "The Modelled Productivity of *Miscanthus* × *giganteus* (GREEF et DEU) in Ireland." *Industrial Crops and Products* 12: 97–109.

Clifton-Brown, J. C., P. Stampfl, and M. B. Jones. 2004. "*Miscanthus* Biomass Production for Energy in Europe and Its Potential Contribution to Decreasing Fossil Fuel Carbon Emissions." *Global Change Biology* 10: 509–518.

Coelho, R. D., J. V. Lizcano, T. H. da Silva Barros, et al. 2019. "Effect of Water Stress on Renewable Energy From Sugarcane Biomass." *Renewable and Sustainable Energy Reviews* 103: 399–407.

Cosentino, S. L., V. Copani, G. Scalici, D. Scordia, and G. Testa. 2015. "Soil Erosion Mitigation by Perennial Species Under Mediterranean Environment." *Bioenergy Research* 8: 1538–1547.

Daryanto, S., L. Wang, and P. A. Jacinthe. 2017. "Global synthesis of drought effects on cereal, legume, tuber and root crops production: A review." *Agricultural Water Management* 179: 18–33.

Davey, C. L., L. E. Jones, M. Squance, et al. 2017. "Radiation Capture and Conversion Efficiencies of *Miscanthus sacchariflorus*, *M. sinensis* and Their Naturally Occurring Hybrid *M. x giganteus*." *Global Change Biology. Bioenergy* 9, no. 2: 385–399.

Dietz, K. J., C. Zörb, and C. M. Geilfus. 2021. "Drought and Crop Yield." *Plant Biology* 23, no. 6: 881–893.

Djemel, A., L. Álvarez-Iglesias, R. Santiago, R. A. Malvar, N. Pedrol, and P. Revilla. 2019. "Algerian Maize Populations From the Sahara Desert as Potential Sources of Drought Tolerance." *Acta Physiologiae Plantarum* 41: 1–13.

Dohleman, F. G., and S. P. Long. 2009. "More Productive Than Maize in the Midwest: How Does Miscanthus Do It?" *Plant Physiology* 150, no. 4: 2104–2115.

Dwiyanti, M., J. Stewart, and T. Yamada. 2013. "Bioenergy Feedstocks: Breeding and Genetics." In *Bioenergy Feedstocks: Breeding and Genetics*, 49–66. John Wiley & Sons Oxford, UK.

FAO. 1994. *Soil Map of the World. Revised Legend, With Corrections and Updates*. Reprinted With Updates as Technical Paper 20. ISRIC, Wageningen, The Netherlands.

FAO. 2024. *Agricultural Production Statistics 2010–2023*, 96. FAOSTAT Analytical Briefs. https://openknowledge.fao.org/handle/20.500.14283/cd13755en.

Fernandez, G. C. 1992. "Effective Selection Criteria for Assessing Plant Stress Tolerance." In *Adaptation of Food Crops to Temperature and Water Stress*. AVRDC Publication. https://worldveg.tind.io/record/72511?ln=en&v=pdf.

Fischer, R., and R. Maurer. 1978. "Drought Resistance in Spring Wheat Cultivars. I. Grain Yield Responses." *Australian Journal of Agricultural Research* 29, no. 5: 897–912.

Fox, J., and S. Weisberg. 2018. *An R Companion to Applied Regression*. Sage Publications.

Greef, J. M., and M. Deuter. 1993. "Syntaxonomy of *Miscanthus* × *Giganteus* GREEF et DEU." *Angewandte Botanik* 67: 87–90.

Hastings, A., J. Clifton-Brown, M. Wattenbach, C. P. Mitchell, P. Stampfl, and P. Smith. 2009a. "Future Energy Potential of Miscanthus in Europe." *Global Change Biology. Bioenergy*, no. 2: 180–196.

Hastings, A., J. Clifton-Brown, M. Wattenbach, P. Mitchell, and P. Smith. 2009b. "The Development of MISCANFOR, a New Miscanthus Crop Growth Model: Towards More Robust Yield Predictions Under Different Climatic and Soil Conditions." *Global Change Biology. Bioenergy* 1, no. 2: 154–170.

Hastings, A., M. J. Tallis, E. Casella, et al. 2014. "The Technical Potential of Great Britain to Produce Ligno-Cellulosic Biomass for Bioenergy in Current and Future Climates." *Global Change Biology* 6, no. 2: 108–122.

Heaton, E. A., F. G. Dohleman, and S. P. Long. 2009. "Seasonal Nitrogen Dynamics of Miscanthus × Giganteus and *Panicum virgatum*." *Global Change Biology. Bioenergy* 1, no. 4: 297–307.

Hodkinson, T., E. Petrunenko, M. Klaas, et al. 2016. "New Breeding Collections of *Miscanthus sinensis*, *M. sacchariflorus* and Hybrids from Primorsky Krai, Far Eastern Russia." In *Paper Presented at the Perennial Biomass Crops for a Resource-Constrained World*, edited by S. M. Barth, D. K. Bokern, G. Taylor, and M. B. Jones. Springer.

Holder, A. J., J. P. McCalmont, N. P. McNamara, R. Rowe, and I. S. Donnison. 2018. "Evapotranspiration Model Comparison and an Estimate of Field Scale Miscanthus Canopy Precipitation Interception." *Global Change Biology. Bioenergy* 10, no. 5: 353–366.

Hoover, D. L., L. J. Abendroth, D. M. Browning, et al. 2023. "Indicators of Water Use Efficiency Across Diverse Agroecosystems and Spatiotemporal Scales." *Science of the Total Environment* 864: 160992. https://doi.org/10.1016/j.scitotenv.2022.160992.

Huang, L. S., R. Flavell, I. S. Donnison, et al. 2019. "Collecting Wild *Miscanthus* Germplasm in Asia for Crop Improvement and Conservation in Europe Whilst Adhering to the Guidelines of the United Nations' Convention on Biological Diversity." *Annals of Botany* 124, no. 4: 591–604.

Kalinina, O., C. Nunn, R. Sanderson, et al. 2017. "Extending *Miscanthus* Cultivation With Novel Germplasm at Six Contrasting Sites." *Frontiers in Plant Science* 8: 563.

Kiesel, A., M. Wagner, and I. Lewandowski. 2016. "Environmental Performance of Miscanthus, Switchgrass and Maize: Can C4 Perennials Increase the Sustainability of Biogas Production?" *Sustainability* 9, no. 1: 5.

Kørup, K., P. E. Laerke, H. Baadsgaard, et al. 2018. "Biomass Production and Water Use Efficiency in Perennial Grasses During and After Drought Stress." *Global Change Biology. Bioenergy* 10, no. 1: 12–27.

Lewandowski, I., and A. Heinz. 2003. "Delayed Harvest of miscanthus—Influences on Biomass Quantity and Quality and Environmental Impacts of Energy Production." *European Journal of Agronomy* 19: 45–63.

Linde-Laursen, I. B. 1993. "Cytogenetic Analysis of *Miscanthus* 'Giganteus', an Interspecific Hybrid." *Hereditas* 119: 297–300.

Littleton, E. W., A. B. Harper, N. E. Vaughan, R. J. Oliver, M. C. Duran-Rojas, and T. M. Lenton. 2020. "JULES-BE: Representation of Bioenergy Crops and Harvesting in the Joint UK Land Environment Simulator vn5. 1." *Geoscientific Model Development* 13, no. 3: 1123–1136.

Ma, X. F., E. Jensen, N. Alexandrov, et al. 2012. "High Resolution Genetic Mapping by Genome Sequencing Reveals Genome Duplication and Tetraploid Genetic Structure of the Diploid *Miscanthus sinensis*." *PLoS One* 7, no. 3: e33821. https://doi.org/10.1371/journal.pone.0033821.

Magenau, E., J. Clifton-Brown, D. Awty-Carroll, et al. 2022. "Site Impacts Nutrient Translocation Efficiency in Intraspecies and Interspecies *miscanthus* Hybrids on Marginal Lands." *Global Change Biology. Bioenergy* 14, no. 9: 1035–1054.

Magenau, E., J. Clifton-Brown, C. Parry, et al. 2023. "Spring Emergence and Canopy Development Strategies in Miscanthus Hybrids in Mediterranean, Continental and Maritime European Climates." *Global Change Biology. Bioenergy* 15, no. 5: 559–574.

Malinowska, M., I. Donnison, and P. Robson. 2020. "Morphological and Physiological Traits That Explain Yield Response to Drought Stress in Miscanthus." *Agronomy* 10, no. 8: 1194.

Malinowska, M., I. S. Donnison, and P. R. Robson. 2017. "Phenomics Analysis of Drought Responses in Miscanthus Collected From Different Geographical Locations." *Global Change Biology. Bioenergy* 9, no. 1: 78–91.

Mendiburu, F. d. 2019. "Agricolae: Statistical Procedures for Agricultural Research." https://CRAN.R-project.org/package=agricolae.

Monteith, J. L. 1965. *The State and Movement of Water in Living Organisms. Paper Presented at the 19th Symposia of the Society for Experimental Biology*. Cambridge University Press.

Munns, R., D. Schachtman, and A. Condon. 1995. "The Significance of a Two-Phase Growth Response to Salinity in Wheat and Barley." *Functional Plant Biology* 22, no. 4: 561–569.

Naidu, S. L., S. P. Moose, A. K. AL-Shoaibi, C. A. Raines, and S. P. Long. 2003. "Cold Tolerance of C_4 Photosynthesis in *Miscanthus* × *giganteus*: Adaptation in Amounts and Sequence of C_4 Photosynthetic Enzymes." *Plant Physiology* 132: 1688–1697.

Nakajima, T., T. Yamada, K. G. Anzoua, R. Kokubo, and K. Noborio. 2018. "Carbon Sequestration and Yield Performances of *Miscanthus*× *Giganteus* and *Miscanthus sinensis*." *Carbon Management* 9, no. 4: 415–423.

Nishiwaki, A., A. Mizuguti, S. Kuwabara, et al. 2011. "Discovery of Natural Miscanthus (Poaceae) Triploid Plants in Sympatric Populations of *Miscanthus sacchariflorus* and *Miscanthus sinensis* in Southern Japan." *American Journal of Botany* 98, no. 1: 154–159.

Nunn, C. 2017. *Performance of Miscanthus: Genotype, Environment and Measurement. (PhD)*. Aberystwyth University, Aberystwyth.

Nunn, C., A. F. S. Hastings, O. Kalinina, et al. 2017. "Environmental Influences on the Growing Season Duration and Ripening of Diverse *Miscanthus* Germplasm Grown in Six Countries." *Frontiers in Plant Science* 8: 907.

Ortiz, R., H.-J. Braun, J. Crossa, et al. 2008. "Wheat Genetic Resources Enhancement by the International Maize and Wheat Improvement Center (CIMMYT)." *Genetic Resources and Crop Evolution* 55: 1095–1140.

Peters, W., A. Bastos, P. Ciais, and A. Vermeulen. 2020. "A Historical, Geographical and Ecological Perspective on the 2018 European Summer Drought." *Royal Society* 375: 20190505.

Pogson, M., A. Hastings, and P. Smith. 2013. "How Does Bioenergy Compare With Other Land-Based Renewable Energy Sources Globally?" *Global Change Biology. Bioenergy* 5, no. 5: 513–524.

Price, L., M. Bullard, H. Lyons, S. Anthony, and P. Nixon. 2004. "Identifying the Yield Potential of *Miscanthus* x *giganteus*: An Assessment of the Spatial and Temporal Variability of M. X *Giganteus* Biomass Productivity Across England and Wales." *Biomass and Bioenergy* 26, no. 1: 3–13.

R Core Team. 2024. *R: A Language and Environment for Statistical Computing*. R Foundation for Statistical Computing. https://www.r-project.org/.

Ramirez-Villegas, J., J. Watson, and A. J. Challinor. 2015. "Identifying Traits for Genotypic Adaptation Using Crop Models." *Journal of Experimental Botany* 66, no. 12: 3451–3462.

Reynolds, M., and P. Langridge. 2016. "Physiological Breeding." *Current Opinion in Plant Biology* 31: 162–171.

Rötter, R. P., F. Tao, J. G. Höhn, and T. Palosuo. 2015. "Use of Crop Simulation Modelling to Aid Ideotype Design of Future Cereal Cultivars." *Journal of Experimental Botany* 66, no. 12: 3463–3476.

Russell, L., S. Henrik, L. Jonathon, B. Paul, and H. Maxime. 2018. "Estimated Marginal Means, Aka Least-Squares Means." *American Statistician* 34: 216–221.

Semagn, K., Y. Beyene, M. L. Warburton, et al. 2013. "Meta-Analyses of QTL for Grain Yield and Anthesis Silking Interval in 18 Maize Populations Evaluated Under Water-Stressed and Well-Watered Environments." *BioMed Central. Genomics* 14: 1–16.

Shanmuganathan, M., and R. Sudhagar. 2021. "Chapter-2 the Prospective of Wide Hybridization: A Sugarcane Perspective." In *Advances in Genetics and Plant Breeding*, 17. AkiNik Publications.

Shepherd, A., D. Awty-Carroll, J. Kam, et al. 2023. "Novel Miscanthus Hybrids: Modelling Productivity on Marginal Land in Europe Using Dynamics of Canopy Development Determined by Light Interception." *Global Chnage Biology. Bioenergy* 15, no. 4: 444–461.

Shepherd, A., E. Littleton, J. Clifton-Brown, M. Martin, and A. Hastings. 2020. "Projections of Global and UK Bioenergy Potential From *Miscanthus* × *Giganteus*—Feedstock Yield, Carbon Cycling and Electricity Generation in the 21st Century." *Global Chnage Biology. Bioenergy* 12, no. 4: 287–305.

Smith, R. P., and J. Boardman. 2025. "Muddy Flooding From Soil Erosion Associated With Maize Cultivation: A Case Study From East Devon, UK." *Soil Use and Management* 41, no. 1: e70038.

Stavridou, E., R. J. Webster, and P. R. Robson. 2019. "Novel Miscanthus Genotypes Selected for Different Drought Tolerance Phenotypes Show Enhanced Tolerance Across Combinations of Salinity and Drought Treatments." *Annals of Botany* 124, no. 4: 653–674.

Stephens, W., T. Hess, and J. Knox. 2001. "Institute of Water and Environment." *In Review of the Effects of Energy Crops on Hydrology*. Cranfield University.

Stewart, J. R., Y. Toma, F. G. Fernandez, A. Nishiwaki, T. Yamada, and G. Bollero. 2009. "The Ecology and Agronomy of *Miscanthus sinensis*, a Species Important to Bioenergy Crop Development, in Its Native Range in Japan: A Review." *Global Chnage Biology. Bioenergy* 1: 126–153.

Sun, X., T. Peng, and R. Mumm. 2011. "The Role and Basics of Computer Simulation in Support of Critical Decisions in Plant Breeding." *Molecular Breeding* 28: 421–436.

Swarup, S., E. J. Cargill, K. Crosby, L. Flagel, J. Kniskern, and K. C. Glenn. 2021. "Genetic Diversity Is Indispensable for Plant Breeding to Improve Crops." *Crop Science* 61, no. 2: 839–852.

Taylor, S. H., B. S. Ripley, T. Martin, L. A. De-Wet, F. I. Woodward, and C. P. Osborne. 2014. "Physiological Advantages of C4 Grasses in the Field: A Comparative Experiment Demonstrating the Importance of Drought." *Global Change Biology* 20, no. 6: 1992–2003.

Thiry, A. A., P. N. Chavez Dulanto, M. P. Reynolds, and W. J. Davies. 2016. "How Can We Improve Crop Genotypes to Increase Stress Resilience and Productivity in a Future Climate? A New Crop Screening Method Based on Productivity and Resistance to Abiotic Stress." *Journal of Experimental Botany* 67, no. 19: 5593–5603.

Van der Werf, H. M. G., W. J. M. Meijer, E. W. J. M. Mathijssen, and A. Darwinkel. 1993. "Potential Dry Matter Production of *Miscanthus sinensis* in The Netherlands." *Industrial Crops and Products* 1: 203–210.

Webster, E. 2020. "Transnational Legal Processes, the EU and RED II: Strengthening the Global Governance of Bioenergy." *Review of European, Comparative & International Environmental Law* 29, no. 1: 86–94.

Weng, T.-Y., T. Nakashima, A. Villanueva-Morales, J. R. Stewart, E. J. Sacks, and T. Yamada. 2021. "Assessment of Drought Tolerance of

Miscanthus Genotypes Through Dry-Down Treatment and Fixed-Soil-Moisture-Content Techniques." *Agriculture* 12, no. 1: 6.

Wickham, H., and C. Sievert. 2009. *ggplot2: Elegant Graphics for Data Analysis*. Vol. 10. Springer.

Xi, Q., and S. Jezowkski. 2004. "Plant Resources of Triarrhena and *Miscanthus* Species in China and Its Meaning for Europe." *Plant Breeding and Seed Science* 49: 63–77.

Zhang, B., A. Hastings, J. Clifton-Brown, D. Jiang, and A. P. Faaij. 2020a. "Modelled Spatial Assessment of Biomass Productivity and Technical Potential of *Miscanthus× giganteus*, *Panicum virgatum* L. and Jatropha on Marginal Land in China." *GCB Bioenergy* 12: 328–345.

Zhang, B., A. Hastings, J. Clifton-Brown, D. Jiang, and A. P. Faaij. 2020b. "Spatiotemporal Assessment of Farm-Gate Production Costs and Economic Potential of *Miscanthus× giganteus*, *Panicum virgatum* L., and Jatropha Grown on Marginal Land in China." *GCB Bioenergy* 12, no. 5: 310–327.

Zhang, H., J. Li, Q. Zhu, et al. 2025. "Linkage Drag and Domestication Syndrome: The Genetic Lessons From Rice Evolution." *Molecular Plant Breeding* 16: 13–23.

Supporting Information

Additional supporting information can be found online in the Supporting Information section. **Figure S1:** Soil moisture content as measured daily at depths of 25 and 75 cm below the irrigated and rain-fed plots of three genotypes over three years in the WATBIO trial at JKI Braunschweig. Data synchronised by adjustments of a maximum of 3.3% on the 1st of January 2018. Standard error bars, $n = 3$. **Figure S2:** Stem counts as calculated from plants in the centre of the plot. Over three years for the WATBIO field trial located in JKI—Braunschweig, Germany. Only two counts were done in 2018 at the start and the end of the year. Error bars ±1 SE, $n = 4$. **Figure S3:** Dynamics of light interception (percentage of incident radiation intercepted by the canopy) for nine genotypes, over three years for the WATBIO field trial located in JKI—Braunschweig, Germany. Error bars ±1 SE, $n = 4$.